rijkswaterstaat
dienst getijdewateren
bibliotheek
e-1316g 430

MOSES : MODEL OF THE SCHELDT ESTUARY

ECOSYSTEM MODEL DEVELOPMENT UNDER SENECA

$$FluxO_2 = \alpha * [J_1(1 - e^{-\sqrt{\frac{k_1}{D_e}} z_n}) + J_2(1 - e^{-\sqrt{\frac{k_2}{D_e}} z_n})]$$

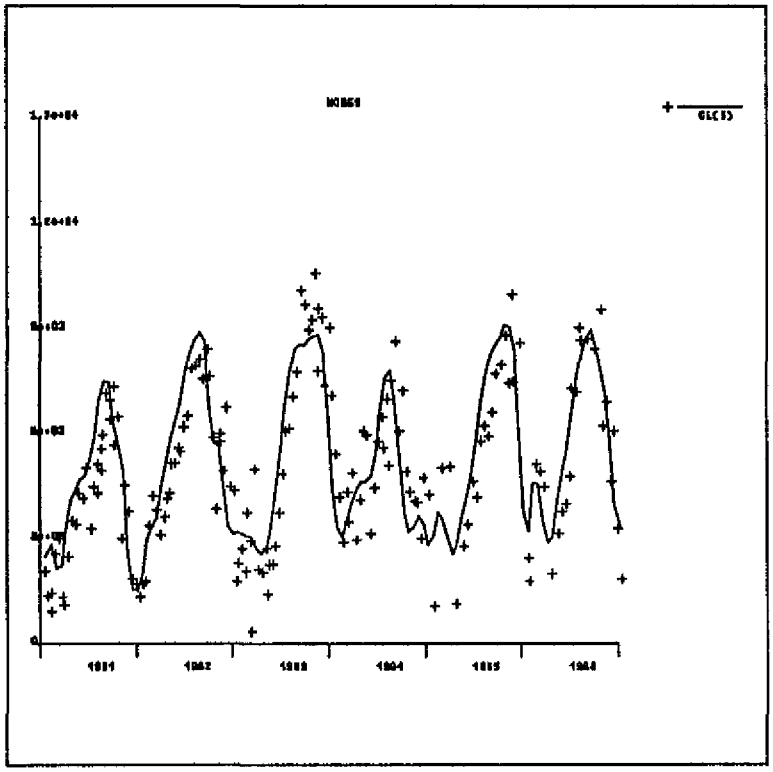

$$\frac{\partial s}{\partial t} = -U\frac{\partial s}{\partial x} + E_x\frac{\partial^2 s}{\partial x^2} - Ks$$

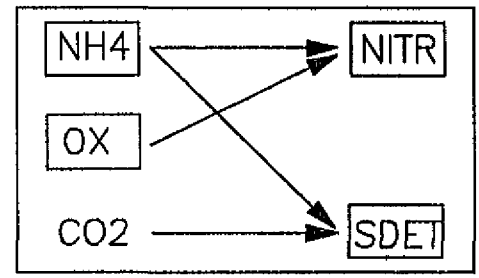

Karline Soetaert, Peter M.J. Herman, Huub Scholten

Ecolmod rapport EM-3

NIOO-CEMO Centrum voor Estuariene en Mariene Oecologie
Vierstraat 28, 4401 EA Yerseke

MOdel of the Scheldt EStuary - Ecosystem model development under SENECA.

by Karline Soetaert, Peter M.J. Herman & H. Scholten.

Concept rapport

Project ECOLMOD
Contract nr. DY-281
Project leaders J. Schobben & P.M.J. Herman
Supervising group R. Duin, B. Haenen, P.M.J. Herman, B.J. de Hoop, J. Schobben, M. vd. Tol
Payed by D.G.W.

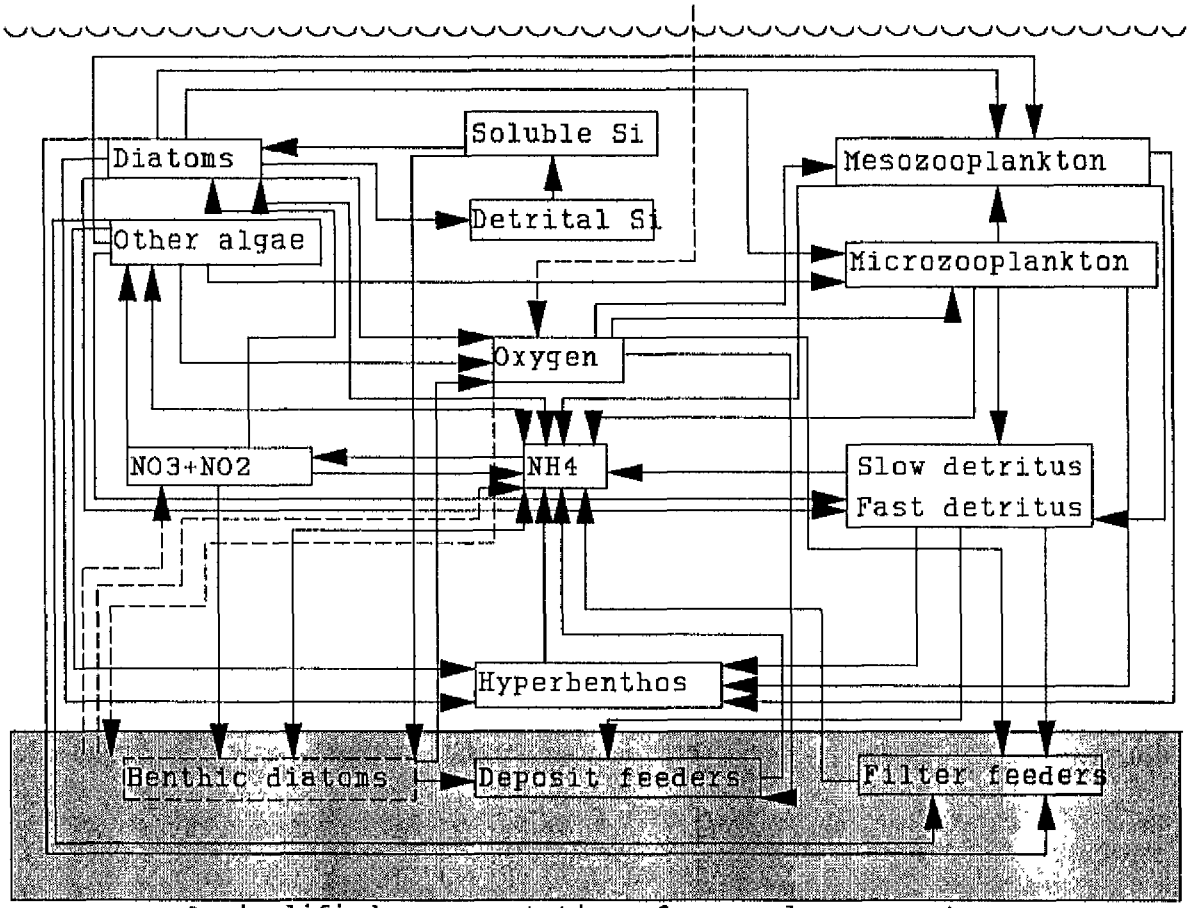

A simplified representation of a complex ecosystem.

Table of contents

1 Introduction

Mathematical models are useful abstractions of the real world as they aid in the understanding and quantification of complex relationships that cannot be gained at first sight. Moreover, mathematical model formulation is the simplest way to achieve quantitative predictions. Global ecosystem models can provide a framework, starting from which new and complex hypotheses can be tested. One can view such a model as an expert system, summarizing knowledge on small parts of the ecosystem into a mathematical frame and connecting all this knowledge into one functional unit.
In recent years much work has been devoted to the modeling of the aquatic ecosystems of the Dutch Delta. Integrated models of the Grevelingen (Vries et al., 1988) and the Oosterschelde (Klepper, 1989; Klepper et al., submitted) have been developed and were logical consequences of the scientific effort directed towards these regions. Recently the scientific emphasis has been on the only true remaining estuary of the Delta region, the Westerschelde. The global ecosystem model MOSES (MOdel of the Scheldt EStuary) that is presented here can be viewed as the first attempt to summarize scientific ecosystem knowledge into one integrated model. Opposite to other simulation models of the Westerschelde (SAWES, 1991), in MOSES the biological processes are emphasized.

Although each ecosystem exhibits its own unique features, several phases of the modeling exercise are redundant and can be handled by more general routines. Therefore a simulation package (SENECA, de Hoop et al., 1992) has been developed at the Delta Institute for Hydrobiological Research at Yerseke, the Netherlands, in cooperation with and financed by the Tidal Waters Division of the Ministry of Transport and Public Works, The Hague. SENECA takes care of universal modeling routines as input-output management, calibration, sensitivity analysis and numerical integration in time. The development of the ecosystem model MOSES was viewed as a test of this simulation package.

2 The Scheldt estuary

2.1 Physical characteristics

The Scheldt Estuary is situated in the Delta region (S.W. Netherlands). It consists of the tidal part of the river Scheldt (reaching up to Gent) and the so called Westerschelde, the southernmost sea-arm in this region. The river Scheldt flows from France through Belgium into the (Dutch) Westerschelde. The river outflow is 100 to 150 $m^3 s^{-1}$, which is relatively small compared to tidal exchange (Van Eck et al., 1991). The Scheldt water is polluted by (largely untreated) domestic and industrial waste water, originating from densely populated areas in Northern France and the Belgian cities of Ghent, Brussels, and Antwerp (Heip, 1988; Hummel et al., 1988; Herman et al., 1991; Van Eck and De Rooij, 1990; Heip, 1989; Duursma et al., 1988). The pollution consists mainly of organic matter of domestic origin (BOD), nutrients (N, P, Si), heavy metals and micro-organics.

Several authors divide the Scheldt Estuary into subsystems: a marine

zone (lower estuary), a brackish zone (upper estuary) and a fluvial zone (tidal river).

The marine zone consists of deep and large channels separated by large sand banks (Heip, 1989). The morphology of this part of the estuary ensures that the water column is completely mixed. The water in the upper estuary flows along a single channel and mixing is not complete here. Small lateral and vertical gradients in salinity exist (Peters & Sterling, 1976). In the fluvial zone the relatively small cross sectional area and the large tidal effects enhance mixing. A zone of high turbidity is found near Antwerpen.

Estuaries are dynamical systems in which transport of substances plays a major role. Although the magnitude of transport of the Scheldt estuary to the North Sea is less than the river Rhine, it is still substantial. A major part of the substances enters the estuary as organic compounds which decompose by an intense heterotrophic bacterial activity (Heip, 1989), resulting in low oxygen concentrations and high dissolved nutrient concentrations. These nutrients leave the estuary at the North Sea boundary. Besides the transport of dissolved substances, large amounts of particulates enter the estuary, both from sea and land (Van Eck and de Rooij, 1990). The flow of salt water close to the bottom transports inorganic clay particles upstream, while the river carries large amounts of organic particles with associated metals and micro-organics. Both particle flows meet in the brackish zone and settlement occurs at the turbidity maximum. Beside these natural processes, man-made dredging activities profoundly change the particulate flux of the estuary (Belmans, 1988).

2.2 Biological characteristics

Two different food chains are distinguished in the Westerschelde estuary. In the brackish part where the load of allochtonous organic carbon is high, a detritus-based food web prevails (Hummel et al. 1988). This detrital carbon is of fluvial origin or consists of locally disposed domestic wastes. In the marine part where detritus concentrations are lower, the autochtonous primary production drives the food chain (Hummel et al., 1988).

Primary production is highest in the zone of maximum turbidity, near Antwerp: it is estimated to be 1000 to 2000 gC m^{-2} y^{-1} (Van Spaendonk et al., submitted) and is at least partly contributed by fresh water algae. The oxygen conditions in this region are badly deteriorated due to intense bacterial decomposition of organic compounds (Heip, 1989). Consequently, the large zooplankters which are sensitive to good oxygen conditions have their maximum biomass somewhat downstream from this algal and bacterial peak (Soetaert & Van Rijswijk, submitted). In the marine part of the estuary the primary production is an order of magnitude less than in the region near Antwerp.

Zoobenthos requires relatively good oxygen availability year round. Therefore biomasses are relatively high in the seaward outer estuary where oxygen concentrations are always high (Ysebaert & Meire, 1990).

Besides the above mentioned zooplankton and zoobenthos, a third group of consumers have to be mentioned here: hyperbenthos. Their role in the Scheldt ecosystem has been investigated recently (Mees & Hamerlynck, submitted).

The effect of other representatives of higher trophic levels (birds and fishes) is probably neglegible, as shown in the steady state model of the Westerschelde (Klepper and Stronkhorst, 1988).

2.3 Chemical characteristics

Several gradients in concentrations of chemical substances exist in the estuary.

Salinity decreases from the seaward boundary (32 ‰) to about zero (depending on the season) in the upper estuary.

The oxygen gradient is very pronounced: in the marine part the water is always close to saturation, while near-anoxia prevails in the maximum turbidity zone. The oxygen concentration is very important as it controls which electron acceptor will be used for the decomposition of organics. It also determines the nitrification-denitrification process, important in the nitrogen cycle. Oxygen concentration within the sediment is even lower than in the water column. Primary production will increase oxygen concentration but reaeration of oxygen from the athmospere will certainly be the major source of oxygen.

Nutrients are always available in high concentrations. No nutrient limitation will therefore reduce primary production, except perhaps dissolved silicates in the outer estuary which could limit diatom growth.

The chemistry of the estuary is very complex. Not only because so many processes are involved, but also the different time scales on which these processes occur. These range from months (decay of relatively refractory detritus) to seconds for some chemical transformations.

3 Existing simulation models of the Scheldt estuary

3.1 Model complexity and integration of different types of models

Model complexity comes in different disguises and every modeling discipline has a characteristic level of complexity.

Hydrodynamic models for instance have a very high resolution in time and space, but they are relatively simple in the amount of processes and state variables which describe the state of the system. They are based on (well known) physical laws and identification of the major aspects is relatively easy. Hydrodynamic models are usually run to calculate conditions for one or perhaps several days.

Ecological and chemical models on the other hand are simple where they show very low spatial (order of magnitude 10000 m) and temporal (time steps of one day) resolution. Their complexity is caused by the number of state variables and processes that have to be described and the variable time scale of the biological and chemical processes (bacterial turnover rates of hours, zoobenthos recruitment in several years). Moreover, many process parameters are not well known and can sometimes hardly be measured (for technical or economical reasons).

Notwithstanding the above mentioned differences, hydrodynamic models can contribute substantially to the quality of ecological and chemical models. Results of the former type of models can be used as input for the latter when averaged over longer periods of time and space.

3.2 Hydrodynamic models

A whole series of hydrodynamic models exist for the Scheldt estuary:

IMPLIC, WAQUA, ZUNOWAK/GENO (2DH water), TRISULA (3D water) and a hydrodynamical model of the Scheldt estuary developed for the MArine Science and Technology (MAST) project of the EC. The latter model will produce output of dispersive flows which will be compared with flows calculated within MOSES. The residence time of (moving) pelagic compartments above the (fixed) bottom compartments will also be estimated with this model. This is necessary for the coupling of benthic and pelagic processes.

3.3 Heavy metals and organic micro pollutants

Other studies (SAWES, 1991; HISWA) aim at modeling the processes associated with heavy metals and their speciation in the Scheldt estuary. SAWES and DELWAQ SLIB include modeling of organic micro pollutants. MOSES does not intend to repeat this effort, but future incorporation of this is not excluded.

3.4 Ecology

Some model studies have ecological impact. In a steady state model of the Scheldt estuary ecosystem (Klepper and Stronkhorst, 1988) balanced carbon flows on a year-averaged base are calculated. From this study it can be concluded that, given certain estimates of biomasses and process rates and their associated uncertainties, a closed budget is possible.

In the water quality model SAWES (SAWES, 1991) some attention has been paid to ecological processes. The description of phytoplankton primary production has been incorporated to be able to model oxygen conditions in the estuary. Model descriptions are based on the North Sea phytoplankton model DYNAMO (WL, 1989). Processes related to higher trophic levels are omitted but biochemical processes associated with decomposition and heavy metal speciation are emphasized.

Billen et al. (1986) developed a model for the calculation of a nitrogen budget of the Schelde.

4 Ecosystem MOdel of the Scheldt ESstuary: MOSES

4.1 Model aims

If an ecological model is to be of any value, it has to meet the aims for which it is developed. In the case of MOSES these aims are:

1. To provide a mathematical description of the Scheldt estuary ecosystem.
2. To determine the origin and the fate of organic carbon in the estuary, its role in the foodweb, and especially the relative importance of phytoplankton primary production.
3. To test the possibilities of SENECA as a model development tool.

4.2 Schematization

Tidal effects in the Schelde reach up to Gent, but for practical reasons

only the estuarine system downstream of Rupelmonde (Figure 2.) will be modeled.

4.2.1 Pelagic schematization

In large ecosystem models the area is subdivided in a number of compartments which are supposed to be more or less homogeneous with respect to the modeled processes. One of the restrictions on the number of compartments is that they should be sufficiently large such as to allow a reasonably large time step, however without the risk of an untolerably large numerical dispersion (Thomann & Mueller, 1987). Moreover, as the spatial resolution is increased (i.e. the separation between grid points reduced), the time step must be decreased to maintain computational stability, at least for the explicit schemes that are generally used (Pond & Pickard, 1989). Thus one can easily see why a desire to improve the resolution of a model is limited by the speed of the computer.

For practical reasons, the one-dimensional schematization of the SAWES model (SAWES, 1991) is implemented in MOSES. In the SAWES model, the part downstream from Rupelmonde is divided into fourteen compartments (Figure 1.). There are two boundaries (sea and freshwater boundary). As numerical instability was very high in the small compartments 6 and 7 of the SAWES model (van Eck, pers. comm.) these were combined into one compartment. Thus thirteen pelagic MOSES compartments as opposed to 14 SAWES compartments are distinguished (Figure 2.).

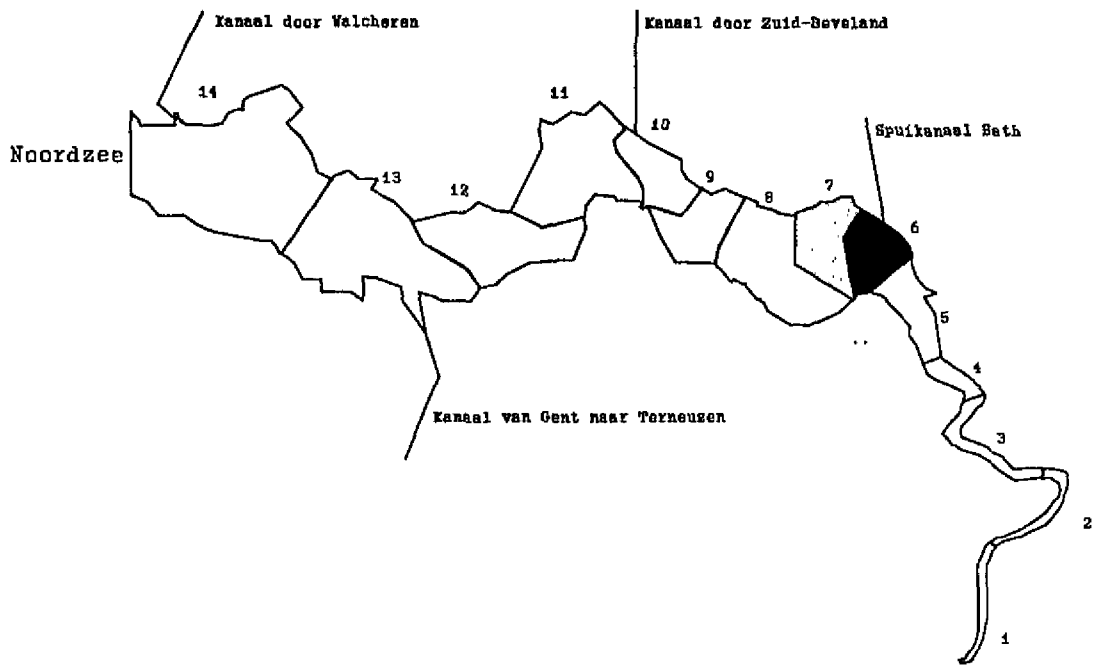

Figure 1. Spatial schematization in SAWES.

4.2.2 Benthic schematization

Whereas the Belgian part of the Schelde is composed of only one channel, in the Dutch part gullies cut through subtidal areas and are intertwined. Mudflats are present in some areas. These different morphological entities (Figure 3.) have a different impact on the ecosystem and this has to be

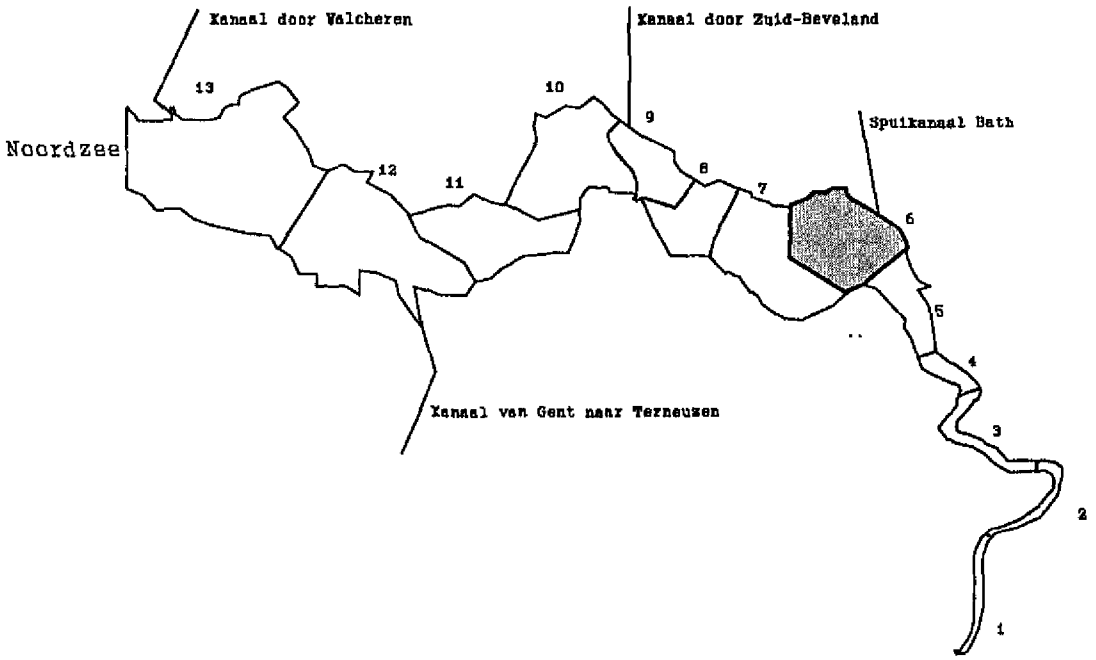

Figure 2. Spatial schematization in MOSES.

translated into MOSES (see also section 4.4.12.)

<u>Intertidal compartments</u>

The tidal flat schematization was designed completely independent of the pelagic compartments. Instead more natural subdivisions were implemented (Figure 4.). They consist of:

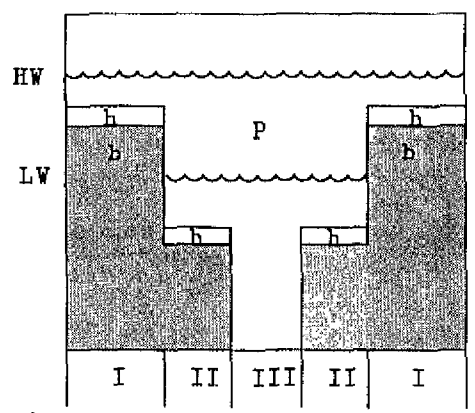

Figure 3. Bottom morphology and biological units. I=tidal flat, II=subtidal, III=gully, HW=high water, LW=low water. b=benthos, p=plankton, h=hyperbenthos.

Compartment number	surface 10^4 m^2	tidal flats (if names exist)
1	1420	Plaat van Breskens, Hooge Platen, Lage Springer
2	440	Subtidal area from Breskens to Terneuzen
3	250	Subtidal area from Sloehaven to Ellewoutsdijk
4	930	Suikerplaat, Middelplaat
5	400	Slikken van Everingen, Plaat van Baarland
6	920	Rug van Baarland, Brouwerplaat, Molenplaat
7	420	Eastern part of Plaat van Ossenisse
8	570	Subtidal area from Terneuzen to Perkpolder
9	1560	Subtidal area from Kruiningen to Bath, plaat van Walsoorden, platen van Valkenisse
10	1530	Subtidal area from Perkpolder to Doel, Subtidal zone of Saeftinghe
11	280	Area from Bath to Zandvliet, Ballastplaat
12	140	Area from Zandvliet to Boudewijnsluis + area from Doel to Kallo
13	90	Area from Boudewijnsluis to Antwerpen

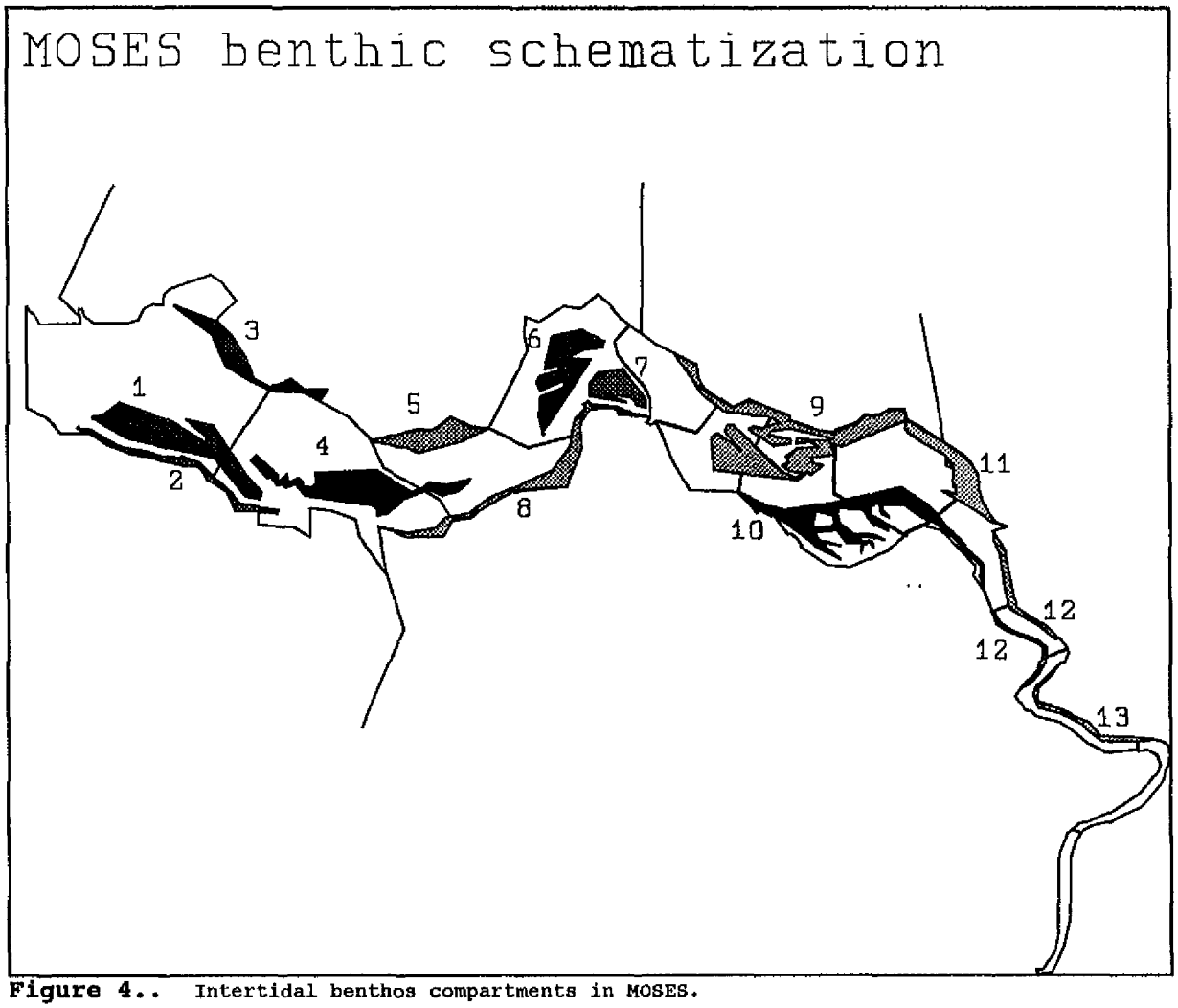

Figure 4.. Intertidal benthos compartments in MOSES.

Subtidal compartments

Subtidal areas are no such obvious morphological entities as the intertidal. They were considered to be associated to the pelagic compartments and defined as the fraction of total bottom surface in the pelagic compartment that is deeper than the subtidal and less deep than 10 meter.

4.3 State variables

4.3.1 Introduction

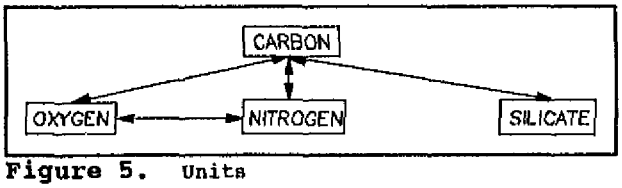

Figure 5. Units

In concordance with the model aims MOSES is in essence a carbon model and state variables are - whenever possible - expressed in units of Carbon (g C/m^3 for pelagic, g C/m^2 for benthic variables). Silicate is modeled as a particulate and a dissolved fraction to allow for processes which are important for diatoms. Also connected via stoichiometric equations is the nitrogen cycle, where two state variables are modeled (ammonia, nitrate+nitrite). Oxygen consumption and oxygen production are

calculated from each process through conversion factors (carbon to oxygen in primary production-respiration processes, nitrogen to oxygen in nitrification-denitrification processes) (Figure 5.).

Two different stages in the modeling process can be discerned: a preliminary model with forcing functions for several biomasses of higher trophic level groups and a final model.
Following state variables will ultimately be incorporated into MOSES:

state variables water column:	Units	Acronym
freshwater diatoms	g C/m^3	FRDIA
freshwater flagellates	g C/m^3	FRALG
brackish and marine diatoms	g C/m^3	BRDIA
brackish and marine flagellates	g C/m^3	BRALG
meso-zooplankton	g C/m^3	ZOO
micro-zooplankton (+ benthic larvae)	g C/m^3	MIC
fast-decay detritus	g C/m^3	FDET
slow-decay detritus	g C/m^3	SDET
detrital silicon	g Si/m^3	DETSi
dissolved silicon	g Si/m^3	SOLSi
nitrate and nitrite (NO_3+NO_2)	g N/m^3	NITR
ammonium (NH_4)	g N/m^3	NH4
oxygen (O_2)	g O/m^3	OX
chlorides	g Cl/m^3	CL
hyperbenthos	g C/m^2	HYP

state variables bottom (intertidal areas):		
benthic diatoms	g C/m^2	DIAB
suspension feeders	g C/m^2	BSUSP
deposit feeders	g C/m^2	BDEP

Forcing functions	
seston	g/m^3
water temperature	°C
irradiation	W/m^2
daylength	hours

The relation between the state variables of the model will be defined in section 4.4.

4.3.2 Phytoplankton

Four different phytoplankton pools are distinguished: brackish + marine and freshwater algae which are either diatoms or non-diatoms (mainly flagellates).
Diatoms are discriminated from other algae as they contain large amounts of silicate. They usually bloom in spring, which causes silicate depletion after which they are replaced by flagellates in summer (Parsons et al., 1984). The two phytoplankton groups were separated to allow for the incorporation of silicate limitation in the model.
Freshwater and marine + brackish algae are discriminated in order to model a 'salinity-stress' mortality.

4.3.3 Zooplankton

Traditionally the zooplankton is divided into size-based groups: micro-, meso- and macrozooplankton.
In MOSES only the micro- and the meso-zooplankton are modeled. The first group consists of protozoa and rotifera, the latter group is dominated by copepods (Soetaert & Van Rijswijk, submitted). The macrozooplankton is not included in the model, but exerts its role through grazing on the mesozooplankton (a mortality coefficient). Meroplankton (benthic larvae) is included into the microzooplankton class.
Some ecosystem models use different state variables for one zooplankton group, which correspond more or less with age groups or stages (Kremer & Nixon, 1978). This allows for the time lag that is commonly observed between prey-predator peaks. Moreover, all groups may have different rates and different modes of feeding. In order not to blow up the number of state variables and in view of the adjustable time step in SENECA (the model of Kremer & Nixon requires time steps of one day), we will do at first with one state variable per group. If however this scheme fails to reproduce the zooplankton dynamics adequately then the mesozooplankton state variable can be subdivided into age classes.

4.3.4 Bacteria

As in SMOES (Klepper, 1989), bacteria are not modeled separately in MOSES. Instead they are included in the detritus fraction and the mineralization is described as simple first-order processes.

4.3.5 Detritus

The detritus in rivers and estuaries is a complex mix of biochemicals with oxidation rates ranging from hours to thousands of years (Spitzy & Ittekot, 1991). For modeling purposes, the degradability of organic matter is an important factor as it affects not only the regeneration of nutrients but also profoundly changes the oxygen conditions of the environment.
The labile organic matter in natural water is present as a continuum of biodegradabilities and C/N content (Garber, 1984). In MOSES two detritus state variables with different biodegradabilities and C/N content are distinguished, as recommended in Lancelot & Billen (1985) and Billen & Lancelot (1988). It are slowly and fast decaying detritus. A third part of organic matter is refractory, i.e. unsusceptible to degradation in the time course of about 1 year. This refractory detritus is not modeled but when it is formed it is supposed to join the pool of suspended matter and is thus considered as a loss term.
In an attempt to account for different degradabilities, modelers can also resort to the description of detrital Carbon and detrital Nitrogen. Decomposition is then a function of the N/C ratio and proceeds somewhat faster for N-detritus than for C-detritus. This approach has for instance been adopted in GREWAQ (De Vries et al., 1988), a model for lake Grevelingen. Although stoichiometric equations become much simpler in this way, it has some important disadvantages. Fast responses of the ecosystem to highly degradable excretions for instance cannot be modeled in this way as the excretions join the common pool and will be decayed with an average (low) rate.
The separation into a fast-decaying and a slow-decaying detritus fraction also allows for the simulation of the different role of the water column versus the sediment in mineral regeneration. Fast decay will be situated predominantly in the water phase and is important for the sustaining of

primary production. Slowly decomposing organic matter will accumulate into the sediment. Thus the sediment becomes an important reservoir of minerals and will be responsible for the gradual increase in nutrient level of the water in winter and consequently of the phytoplankton bloom in spring (Billen & Lancelot, 1988).

The (arbitrary) distinction between dissolved and particulate organic matter is not made here. Both the slow and fast decaying detritus fractions consist of a dissolved and a particulate phase.

4.3.6 Dissolved inorganic nitrogen

Although nitrogen is not a limiting nutrient in the Schelde, there are some compelling reasons to incorporate the nitrogen cycle into the model.

At first, implications of future reductions of the nitrogen load of the water can not be assessed if nitrogen is not modeled (could nitrogen eventually become the limiting nutrient if waste discharges are sufficiently treated ?).

In most ecosystems denitrification and ammonification (the reduction of nitrate) is a process which occurs in the anaerobic layers of the sediment, while nitrification (the oxidation of ammonium) occurs in the aerobic bottom layer and in the water column. This also holds for the well aerated parts in the Westerschelde. In the more upstream part where (near) anoxic conditions in the watercolumn prevail, however, denitrification occurs essentially in the pelagic realm. The magnitude of this denitrification is not unimportant as it ultimately determines the amount of nitrogen which is lost from the ecosystem to the atmosphere. Obviously, the more pronounced this process, the less will be the nitrogen fertilisation of the continental shelf. Some model studies even predict that ameliorating the oxic conditions of the Westerschelde (and thus lowering the denitrification) would tend to increase the discharge of nitrogen to the North Sea, a highly undesirable feature indeed (Billen et al., 1985, 1986). Other studies on the other hand do not confirm this finding (Van Eck et al., 1991). Incorporation of the dissolved nitrogen species into our global ecosystem model (MOSES) can provide an independent test of this hypothesis.

Nitrate and ammonium are not equivalent sources of nitrogen for phytoplankton growth, as ammonium is preferred over nitrate-nitrite (McCarthy et al., 1977). Moreover, some bacteria are consumers of mineral nitrogen and can thus compete with phytoplankton.

Ultimately, the process of nitrification / denitrification not only is determined by oxygen conditions, in its turn it determines the oxygen conditions as nitrification is an oxygen demanding process.

Two DIN state variables are incorporated into MOSES: ammonium and nitrate+nitrite. Nitrite and nitrate are combined into one state variable since nitrite is generally rapidly converted to nitrate. In the Westerschelde, the nitrite concentration usually is less than 5 % of the total nitrate + nitrite pool. Nitrous oxyde and nitrogen gas, both products of denitrification, are not modeled as these are lost to the atmosphere.

4.3.7 Silicate

Silicate is incorporated into MOSES to model DIATOM growth. It consists of a soluble and a detrital fraction.

4.3.8 Oxygen

The Scheldt estuary is characterized by a pronounced gradient in oxygen concentration, ranging from oversaturation in the marine part to near-anoxic conditions in the vicinity of the turbidity maximum near Antwerp. Not only the survival of organisms, but also the type of processes (nitrification-denitrification) strongly depend on the oxygen conditions.

4.3.9 Chlorinity

Modeling chlorinities is especially important for the calibration of the dissolved transport submodel. Once this is done one can do without modeling chlorinities. However, they were kept in MOSES as a permanent check on the dissolved transport. Chlorinities are further used in the description of salinity-stress mortality (but using chlorinity as a forcing function would be equally appropriate !).

4.3.10 Hyperbenthos

Hyperbenthic populations are well developed in the Scheldt estuary, especially in the brackish part where very high biomasses have been reported (Mees & Hamerlynck, submitted).

4.3.11 Phytobenthos

Benthic diatoms are primary producers from intertidal flats and shallow coastal areas.

4.3.12 Zoobenthos

The macrobenthos was subdivided into two feeding groups. Deposit feeders ingest sediment together with organic matter, while suspension feeders capture suspended matter from the pelagic. The meiobenthos is not modeled as such but is included into the deposit-feeding group.

4.4 Processes

4.4.1 Introduction

One of the model aims is the description of the origin and fate of organic carbon in the estuary. Therefore processes related to these objectives (primary production and mineralization) are emphasized.
As the characteristic simulation period will be in the order of years, the time-unit chosen is in days.
The mathematical descriptions in MOSES are kept as simple as possible. We believe it is not appropriate to burden a model in its developmental stage with too much complexity. If a simple -but meaningful !- approach can do the trick the better understandable it will be. If however it turns out that some descriptions are inadequate to reproduce the observations then a more complex description can be at its place.
A simple model requires simple equations and therefore most processes are described as first-order kinetics. Where possible and appropriate, we

adopted the descriptions from the Oosterschelde model SMOES (remark that MOSES is not purely by coincidence an anagram of SMOES !). Some allometric equations (e.g. in the suspension feeders) in SMOES were converted into more straight-forward linear relationships.
Temperature functions were always described by means of a Q10 formulation.

4.4.2 Horizontal transport

Only those state variables which reside in the water column are subjected to passive transport.

Dissolved substances
The exchange of material among compartments and over the boundaries is modeled by means of a tide-averaged, constant volume, advective-diffusive finite difference equation (Thomann & Mueller, 1987). Input to the transport model are (advective) freshwater flows across the compartment interfaces, flows across the boundaries and boundary conditions for the state variables. Dispersive coefficients were calculated by calibration on a conservative substance (salinity). For more information see section 7.3.

Particulate matter
Whereas the net flow of dissolved matter is function of the freshwater discharge in the estuary, particulate matter transport can be entirely independent and even opposite to this seaward transport.
One-dimensional models are rarely fit to simulate mud transport in estuaries and in the Westerschelde estuary particulate transport is further complicated by intense dredging activity (Belmans, 1988).
Although it is not of interest to model this process in MOSES, particulate transport comes into play when modeling substances which do not behave entirely as a dissolved or a particulate substance (e.g. detritus, phytoplankton or zooplankton). As in SMOES (Klepper, 1989) these substances are assigned a partly dissolved, partly particulate behavior and their transport is somewhat inbetween the dissolved and particulate transport. For more information on the implementation of this transport into MOSES, we refer to section 7.3.9.

4.4.3 Vertical transport

Vertical transport consists of sedimentation-resuspension of particulate substances and the exchange of dissolved substances through the sediment-water interface. For the implementation of the former, see section 7.3.10, implementation of the latter is described in detail in section 7.2.

4.4.4 Benthic-pelagic coupling

Describing transport in a constant volume reference frame instead of a fixed frame has some important advantages for pelagic variables: as the frame moves along with the watercolumn, temporal oscillations due to the tides are circumvented. However, problems arise when describing the benthos: oddly enough the bottom now moves with respect to the reference frame with a periodicity of one tidal cycle. Thus a bottom compartment interacts with different pelagic compartments during the course of one tidal cycle. In the coupling of benthic and pelagic processes in MOSES this has to be taken into account and the description has to be general enough such as to be easily ported to other ecosystems.
For each intertidal bottom compartment the fraction of time that each pelagic compartment resides above this bottom will be calculated with the

2D hydrodynamical model of the Scheldt estuary, developed in the lab of Dr. Neves (Portugal). We assume that the degree of interaction of this bottom with the various pelagic compartments is proportionate to this residence time. Bentho-pelagic coupling is then implemented as an array with dimensions (benthic compartments) * (pelagic compartments) representing the relative interaction of each bottom compartment with each pelagic compartment.

The subtidal compartmentalization is conform to the pelagic compartments. Here the pelagic-benthic coupling was done more directly by assuming that during each tidal cycle the more upstream and downstream compartment reside for 25 % above the subtidal compartment, while the corresponding pelagic compartment resides for about 50 % above each subtidal compartment. Thus it is assumed that a pelagic compartment moves in one tidal cycle for a distance of about its length. These approximate interaction coefficients can easily be updated based on the hydrodynamic model.

4.4.5 Organic matter degradation

The schematic representation of this process can be found in Figure 6.
Organic matter degradation is a function of the rate of exoenzymatic hydrolysis which is proportional to the biomass of bacteria (Billen & Lancelot, 1988). As bacteria are not explicitly incorporated into MOSES, it was decided to model mineralization by means of a first order process with respect to the organic load (Streeter & Phelps, 1925). The influence of temperature is modeled by means of a Q10 function. We also included an oxygen-dependent part in the mineralisation, comparable to Baretta & Ruardij (1988). According to these authors the rate of mineralisation depends on the oxygen saturation of the water column (which determines the redox state of the organic matter). This dependency can be expressed by a Michaelis-Menten equation.

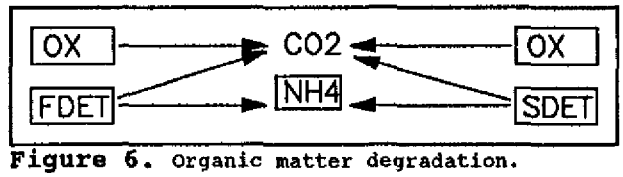

Figure 6. Organic matter degradation.

Organic matter degradation, using nitrate as an electron acceptor will be discussed in the section on nitrification and denitrification. Other anaerobic degradation (using sulphate and lower organic acids as an electron acceptor) is not modeled in MOSES.

4.4.6 Nitrification-denitrification

Nitrification (Figure 7.) is the oxidation of reduced forms of nitrogen to nitrate (Prosser, 1990). It is an aerobic process, mediated by autotrophic bacteria, which obtain energy from oxidation of ammonia and nitrite and obtain cell carbon from carbon dioxide. As bacterial biomass is not modeled as such, the product of nitrification, in terms of carbon will join the slow decaying detritus part.

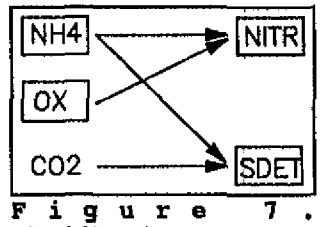

Figure 7. Nitrification

Denitrification (Figure 8.) on the other hand is an anaerobic process carried out by heterotrophic bacteria (Seitzinger, 1988). The products of denitrification are N_2 or N_2O which are lost to the atmosphere. Nitrate reduction can also lead to NH_4^+ formation (about 40 % of all reduction), especially at high organic matter content and low nitrate concentration (Billen & Lancelot, 1988).

Which process is more important strongly depends on the oxygen concentration: nitrification is negatively influenced in reduced conditions (Michaelis-Menten kinetics with respect to oxygen concentration), denitrification is negatively influenced by high oxygen conditions (1-Michaelis-Menten term). Thus denitrification is allowed to take place, even in aerobic conditions. This is because oxygen gradients exist in suspended organic particles of a certain size thus allowing both the processes of nitrification and denitrification to take place at very short distances (GREWAQ, 1988).

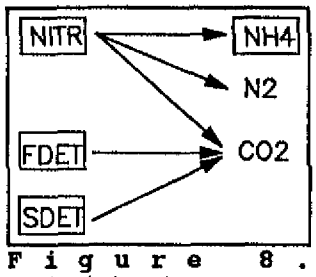

F i g u r e 8 . Denitrification

In the Westerscheldt, nitrification in the sediment is unimportant compared to the water phase (Billen, 1975) whereas denitrification occurs both in the sediment and in the badly aerated water bodies of the Westerschelde (Wollast, 1983).

A simplified approach of modeling nitrification and denitrification can be to assume that all reactions are first-order reactions with respect to the nitrogen source, depending on temperature by means of a Q10 formulation and on oxygen condition by means of a Michaelis-Menten formulation (see above). The amount of detrital carbon can become limiting in case of denitrification and ammonification. This is implemented as a Michaelis-Menten kinetic.

4.4.7 Dissolution of particulate silicate (Figure 9.)

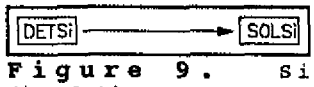

F i g u r e 9 . Si dissolution

This is represented as a first-order process. It is assumed that all detrital silicate resides in the bottom (See also section 4.4.12)

4.4.8 Oxygen exchange water-air interface (Figure 10.)

This will probably be the most important source of oxygen to the watercolumn. It is modeled as in Baretta & Ruardij (1988).

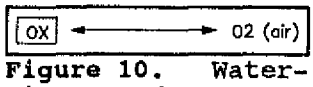

Figure 10. Water-air O_2 exchange.

4.4.9 Phytoplankton processes

4.4.9.1 Gross production

Gross production (Figure 11.) is calculated as the product of maximal production, light limitation and a nutrient limitation factor.

Maximal phytoplankton production

The maximal production rate depends on temperature (Eppley, 1972). This was modeled as a Q10 function in MOSES.

Light-limited phytoplankton growth:

The Eilers-Peeters model (1988) is used to model photosynthesis as a function of light intensity. We implemented the depth-integrated formulation as developed for the Eastern Scheldt by Klepper (1989) into MOSES, taking into account the basin morphology of the Western Scheldt (see sections 7.1, 7.1.2).

Optimal light intensity for photosynthesis is

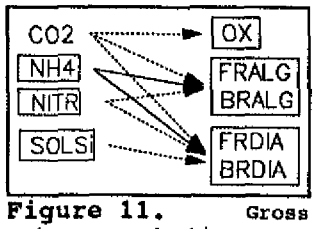

Figure 11. Gross primary production

expressed as a function of temperature (Q10).
Extinction coefficients are calculated as a logarithmic function of suspended matter: E = -3.53 + 4.4 * log(SUSP).
This regression was obtained from Westerschelde data provided by Van Spaendonk (see Addendum 1). Including salinity in the regression did not noticeably ameliorate the fit (r^2 of 0.670 instead of 0.666).

Nutrient limited growth:
Nitrogen can be limiting for non-diatoms; nitrogen and silicate can be limiting for diatoms. Attained production is calculated by the minimum formulation.

In general, ammonium is the preferred form of nitrogen (compared to nitrate and nitrite) for phytoplankton assimilation at concentrations higher than 1 to 2 micromole of ammonium (McCarthy et al., 1977). In MOSES only ammonium is taken up at sufficient ammonium concentration, while in the case of limitation, nitrate and ammonium are taken up simultaneously.

4.4.9.2 Loss terms

As a means of giving diatoms an advantage to algae, a coefficient ARAT was defined (as in Klepper, 1989). This coefficient expresses the higher energy requirements of non-diatom algae compared to diatoms: diatom respiration and excretion is multiplied with this factor to obtain non-diatom rates.

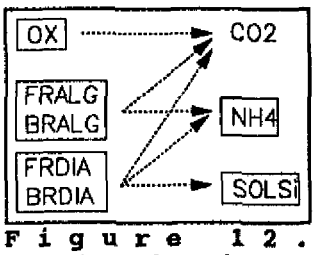

Figure 12. Phytoplankton respiration

Respiration (Figure 12.)
Respiration of algae consists of a maintenance term (depending on temperature) and an activity term (which is a fraction of gross production).

Excretion (Figure 13.)
Extracellular release generally ranges from 0 to 10 % of photosynthetic assimilation (Wetsteijn, 1984). It can however be an important process when primary production is limited by nutrient depletion (Klepper, 1989; Lancelot & Billen, 1985). Thus excretion is modeled as a function of nutrient limitation (as in Klepper, 1989).
The nature of extracellular excretions is quite diverse and they are either very rapidly degradable (hours) or much more refractory.

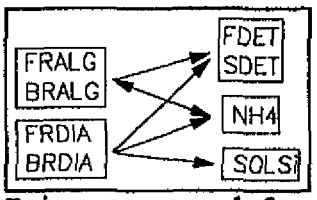

Figure 13. Phytoplankton excretion

Physiological mortality (Figure 14., Figure 15.)
Physiological mortality of algae stands for death due to salinity stress: when freshwater algae are transported into water with too high salinity or when brackish water algae are subjected to too low salinities, they experience a high mortality. This mortality is modeled as a sigmoidal function depending on salinity.

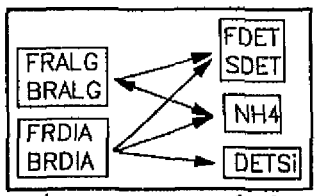

Figure 14. Phytoplankton mortality

Chlorophyll content
Algal biomass most often is expressed in units chlorophyll. Thus a conversion from carbon to chlorophyll has to be

defined. The approach of Klepper (1989) was followed: the chlorophyll content is function of the nutrient and light-limiting functions.

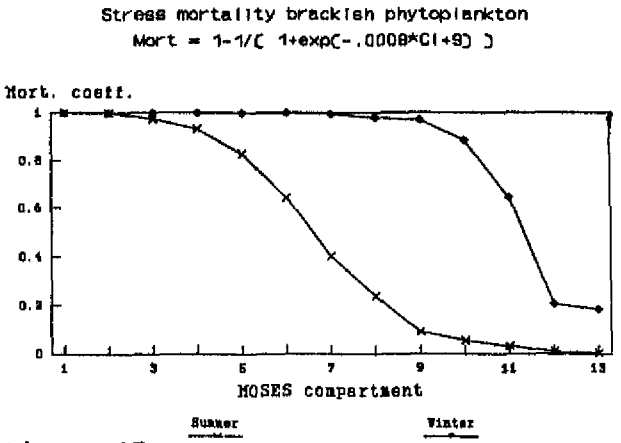

Figure 15. Shape of stress mortality function of brackish water phytoplankton

4.4.10 Zooplankton processes

Grazing

(Figure 16.). The microzooplankton feeds on bacteria, small phytoplankton, small microzooplankton (cannibalism) and detritus. They are themselves grazed upon by larger animals. The microzooplankton thus constitutes an important link in the food web (Fenchel, 1982; Linley et al., 1983; Newell & Linley, 1984), making the smallest edible fractions available to larger heterotrophs. In MOSES the bacteria are not considered separately but included in the detrital carbon fraction. Thus simplified one can state that the microzooplankton eats detritus, phytoplankton and other microzooplankton ; they exhibit no preferences for this or other food source.

The mesozooplankton is dominated by copepods. Two grazing strategies are implemented. In the first strategy they feed preferentially on algae and switch to detritus (and associated bacteria) and microzooplankton or are cannibalistic if algal stocks are insufficient to meet their nutritional requirements. Another strategy is indiscriminate feeding (i.e. at all times feeding is proportionate to the relative food availabilities).

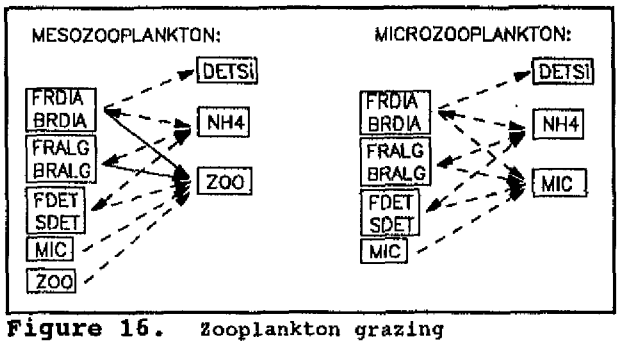

Figure 16. Zooplankton grazing

Maximal food uptake of the zooplankton is modeled as a function of temperature. The actual nutrition is limited by food availability.

Assimilation - faeces production

Assimilation is the part of ingested food effectively taken up by the animal.

A fixed assimilation efficiency is used (.4-.8) (DiToro et al., 1971). What is not assimilated is lost as faeces (Figure 17.).

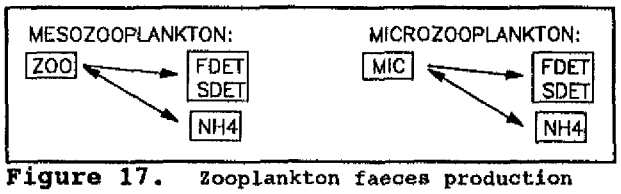

Figure 17. Zooplankton faeces production

Respiration - excretion

(Figure 18.)

The respiration is expressed by means of a Q10 function. Closely coupled to respiration is excretion. The latter process is not independently modeled. Instead it is assumed that the amount of ammonium which is excreted is

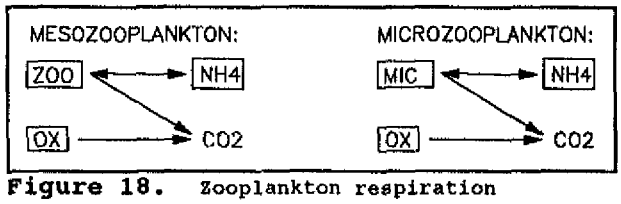

Figure 18. Zooplankton respiration

proportional to the amount of carbon respired (using the nitrogen to carbon ratio of the zooplankton).

Zooplankton mortality (Figure 19.)
Zooplankters have relatively short life-spans. A background mortality, depending on temperature (Q10 formulation) is defined.
Mortality further depends on oxygen concentration: at low oxygen concentration, the mortality is increased. This dependence on oxygen concentration is modeled as a Monod equation with respect to the oxygen saturation. Mesozooplankton is more vulnerable to bad oxygen conditions than microzooplankton: whereas the latter is abundant in the anoxic zone around Antwerp, the former group is nearly absent (Soetaert & Van Rijswijk, submitted).

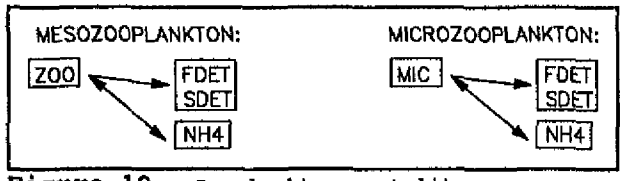

Figure 19. zooplankton mortality

Grazing on the mesozooplankton occurs either by the mesozooplankton itself (cannibalism), by the macrozooplankton, vertebrates and by the hyperbenthos. As the macrozooplankton and vertebrates are not included in the model they exert their role by means of a mortality coefficient which is proportional to the biomass of the mesozooplankton (this is equivalent to a predatory group fluctuating concurrently with the mesozooplankton or also a predatory group with a constant biomass and showing no functional response). In a latter stage a time lag of this coefficient with respect to mesozooplankton biomass can be incorporated.

4.4.11 Hyperbenthos processes

Grazing
(Figure 20.). Mysids, the most abundant hyperbenthic group, are important zooplankton predators in freshwater and marine environments (Rudstam, 1989; Rudstam et al., 1986). When zooplankton is rare, they switch to phytoplankton and detritus (Rudstam, 1989). Ingestion is modeled as a fraction of total body weight.

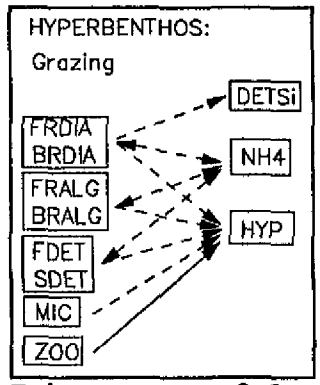

Figure 20.
Hyperbenthic grazing

Assimilation-faeces production
Assimilation is a fraction of the food actually taken up and is rather high in mysids (85 % in Rudstam, 1989). What is not assimilated is lost as faeces.

Respiration-excretion
The respiration rate is expressed as a Q10 function with a weight-specific respiration rate at 5 degrees between .02 and .036 mg O2.g DW^{-1} for various mysid species (Rudstam, 1989). With a dry weight-wet weight ratio of .25, a carbon-to-DW conversion factor of .53 and a oxygen-to-carbon ratio of 4.2, this gives about 3-5% of total body weight. Excretion amounts to about 16 % of assimilated food (Rudstam, 1986). With an ingestion rate of 20 % (10 degrees), an assimilation efficiency of .85 this amounts to about 3 % of body weight at 10 degrees, which confirms well with respiration rates.

Hyperbenthos mortality
Hyperbenthos probably is a food source for demersal fish, which are not

modeled in MOSES. Therefore a mortality coefficient due to predation (fluctuating with hyperbenthos biomass) and a temperature- and oxygen sensitive mortality were defined.

Movement in the estuary

The hyperbenthos takes an intermediate position between the pelagial and the benthos. It is found very near to the bottom but can move independently from the bottom. Research on Westerschelde hyperbenthos (Mees & Hamerlynck, submitted) showed that community patterns are very much fixed in space indicating that movement or active transport is restricted. In MOSES it is assumed that the hyperbenthos is associated with a pelagic compartment. They move with this compartment during the course of one tidal cycle but contrary to the water which is continually moving downstream, the hyperbenthos shows no such passive movement.
Some degree of migration was modeled in MOSES not at least to be able to 'reseed' a compartment with new mysids once they have become extinct. Migration is triggered when oxygen and food conditions deteriorate and occurs as much in the upstream as in the downstream direction. Only a small fraction of hyperbenthos can leave a compartment in one day. Swimming speeds of 1-1.6 cm sec^{-1} have been recorded for mysids (Rudstam, 1989). Provided that they can keep up with this for 24 hours, they can move for about 800-900 meters a day. With a minimal compartment length of 5000 meters they could move from the center of a compartment to the edge in about three days. This seems to be a large overestimation of migratory capacity and .1 was taken as the upper limit of migration (day^{-1}).

4.4.12 Benthic processes

The incoming and outgoing tide in estuaries stands for a large sedimentation-resuspension of material to and from the bottom. Thus there exists a strong coupling of pelagic and benthic processes in estuaries.
In MOSES the gullies, subtidal and intertidal areas are distinguished and different processes are allowed to take place in each subsystem.
The macrobenthos and the meiobenthos are predominantly present in the intertidal areas, relatively few in the subtidal area and almost non-existent in the deep tidal channels (Ysebaert & Meire, 1991; Tulkens, M., 1991). As a first step only the intertidal areas were considered in the zoobenthic submodel. The subtidal areas and the channels were assumed to be inert with respect to the zoobenthic processes.
Benthic primary production is restricted to the zone where light conditions are favourable which in fact limits benthic diatom growth to the intertidal zone.
Decomposition of organic matter and the coupled fluxes of the different nitrogen species and of oxygen to and from the bottom are allowed in the intertidal and subtidal areas only. It is assumed that flushing in the deep channels is strong enough to prevent the organic matter from settling.
As Dissolution of silicate is modeled as a first-rate process with respect to the particulate silicate content it doesn't matter whether this process is modeled in the bottom (where in fact it predominantly is) or in the pelagic phase. Thus in MOSES all detrital silicate is assumed to reside in the bottom compartment below the pelagic compartment where it was produced. This is equal to stating that detrital silicate is a non-moving pelagic state variable.

Summarized this gives

	Intertidal	Subtidal	Gullies
phytobenthos	+	-	-
zoobenthos	+	-	-
N-fluxes	+	+	-
Si-fluxes	-	-	-
O2-fluxes	+	+	-

Nutrient regeneration

In shallow systems, the bottom is important as it is the site of nutrient regeneration for the water column. Sediments can supply up to 70 % of nitrogen requirements of phytoplankton. Moreover, denitrification, which is closely dependent on anaerobic conditions is prominent in the bottom and results in the elimination of nitrogen from the ecosystem. Furthermore, the residence time of part of the organic matter is much longer in the bottom than in the water column and hence nutrient regeneration from the benthos is more steady (Billen & Lancelot, 1988).

Nitrate, ammonium and nitrogen gasses can be released from the sediment. This exchange across the sediment-water boundary is modeled as a function of the nitrate and oxygen concentration of the overlying water and the input of fast and slow decaying detritus as in Lancelot & Billen (1985). See section 7.2 for more information.

Silicate regeneration in the bottom is the same as in the waterphase. It is not modeled separately. Instead, it is assumed that all detrital silicate is in the watercolumn but does not move.

Benthic oxygen flux

Organic matter degradation and nitrification are oxygen-demanding processes and these processes will induce a flux of oxygen from the water phase to the bottom. This bottom oxygen demand was modeled as a flux across the sediment-water interface in the same way as the nitrogen fluxes.
We refer to section 7.2 for more information.

Benthic primary production

Primary production in the benthos occurs only in shallow bottoms and in the top-most layer of the sediment (light conditions). In other words, benthic primary production in the model will be restricted to the intertidal areas. Moreover, the photosynthetic activity is nearly entirely limited to low tide (Scholten et al., in prep). The availability of nutrients is probably sufficient for benthic production, but CO2 in the bottom can become limiting. For production, we used the same formulation as for phytoplankton, except what concerns the integration over depth and the availibility of the limiting nutrients (CO2, Nitrogen and silicate).
The supply of CO2 to the phytobenthos is of crucial importance. Important sources of CO2 are an exchange with the atmosphere when not flooded, mineralization of organic matter, the denitrification process and respiration. We used a constant carbon flux from the atmosphere to the mudflats of 56 mg C/m2/h as in Scholten et al. (in prep.).

Phytobenthos respiration

Respiration is modeled as an activity respiration (fraction of total production is respired) and a temperature dependent rest respiration.
Excretion is coupled to respiration: an equivalent amount of ammonia is released.

Mortality of benthic algae
Deposit feeders graze on benthic algae and indirectly induce some mortality due to their burrowing activity. The latter is modeled as a function of temperature and is a first-order reaction with respect to benthic algae and deposit feeder biomass. Some diatom biomass is lost due to resuspension (action of wind and water). As wind is not available as a forcing function, this mortality is described as proportional to the amount of suspended matter in the water column.

Suspension-feeders
Benthic suspension feeders are non-selective filterers of phytoplankton and suspended detritus. They mainly consist of Cerastoderma edule (cockle) (Ysebaert & Meire, 1990).
The suspension feeders obtain their food (detritus, algae, microzooplankton) from different pelagic compartments (see section 4.4.4). Food uptake is modeled as a clearance rate, which is a function of temperature and is depressed when seston concentrations are high (Klepper, 1989). Unlike SMOES where mean biomass of the suspension feeders is also modeled and where clearance and respiration is an allometric function of mean body weight, in MOSES both are modeled as a first-order process of total biomass. When total clearance exceeds a threshold value, pseudofaeces are released (Klepper, 1989).
Assimilation is a fixed fraction of total ingestion (after exclusion of pseudofaeces production). What is not assimilated is released as faecal matter.
Adult cockles invest once a year a large fraction of their biomass in reproductive output (spawning). In MOSES it was assumed that spawning occurs for the whole month of june (trigger on-off function) and that a fixed part of total biomass is then lost to reproduction.
Respiration and excretion are a function of temperature.
Mortality is modeled as a predation term (proportional to suspension feeder biomass) and a physiological mortality which depends on temperature and oxygen conditions.

Deposit feeders
Deposit feeders (macro- and meiobenthic) feed on benthic diatoms and on benthic detritus. The concentration of benthic detritus can be calculated based on the diagenetic modeling of benthic fluxes (see section 7.2.3). Feeding, respiration and the coupled excretion are a function of temperature and are linearly related to deposit feeder biomass. Predatory mortality is modeled as a mortality coefficient which is proportionate to deposit feeder biomass. A background mortality is a function of temperature (Q10) and of oxygen conditions. A fixed fraction of total ingested biomass is assimilated, the rest is released as faecal matter.

4.4.13 Linking of carbon, silicate, nitrogen and oxygen cycles

Although variables and fluxes in MOSES are (whenever possible) expressed in units of carbon the nitrogen, silicate and oxygen cycle are also included.

Linking carbon with the nitrogen and silicate cycle
Ideally every carbon state variable should have its nitrogen-based and (where appropriate) its silicate-based counterpart. This would allow for the carbon and nutrient ratios to change depending on environmental conditions. A strong advisor against such an approach is the complexity of the resulting model and the loss in speed which inevitably occurs.

Thus one usually couples the various cycles by means of stoichiometric equations (Klepper, 1989; Kremer & Nixon, 1978; DiToro et al., 1971). Each (carbon) state variable has its characteristic nitrogen-to-carbon and silicate-to-carbon ratio, which is invariant in time. Carbon flows are then converted to nitrogen and silicate flows by assuming the appropriate ratios.
However, the conservation of mass has to be assured in some way. In the case of the nitrogen cycle, this is done by adjusting the ammonium pool: whenever matter is transferred to a state variable with a lower nitrogen content, ammonium is released; if the receiving pool has a higher nitrogen-carbon ratio, ammonium is taken up. This appears to be justified as ammonium is the inorganic nitrogen source which is preferentially taken up during photosynthesis. Ammonium is also what is ultimately formed during the mineralisation of detritus and it can be excreted as such by zooplankton. Conservation of silicate is assured by adjusting the dissolved silicate concentration.

Linking with the oxygen cycle
The oxygen cycle is influenced by physical, biological and chemical processes. Degradation of organic matter, respiration and nitrification are processes that consume oxygen. Photosynthesis produces oxygen. Finally, exchange through the water-atmosphere and the water-bottom interface influence the oxygen concentration of the water.
As with nitrogen and silicate, conversion of carbon- and nitrogen flows to oxygen is done by assuming appropriate conversion factors.
For photosynthesis, respiration and mineralization of detritus, a constant conversion factor from carbon to oxygen is assumed. Nitrification, and denitrification are also coupled to the oxygen cycle through fixed stoichiometric values.

4.5 Forcing functions

Forcing functions will be used for irradiation, daylength, water temperature, seston concentrations and -in the preliminary phase- for biomasses of higher trophic levels.

Irradiation data will be used from SMOES, which are daily averages of 6 stations around the Oosterschelde. Irradiation is expressed in W m^{-2}.

Daylength is expressed as a Fourier function:
$DL = 12.49 + 4.45*\sin(2\pi/365 *t-1.406)$
This formula was fitted through values of 1991.

Water temperature is used from SAWES.

Seston concentration is described by means of a function, incorporating effects of freshwater flow (and hence resuspension) and location in the estuary. The function allows for a turbidity maximum at some location, which moves under influence of freshwater flow. It has been derived from seston data from the SAWES data base (see addendum I).

4.6 Boundary conditions

Boundary conditions are required for all state variables that are transported, as one needs to estimate their import into the model. Two

boundaries are defined: the first at Rupelmonde, where the riverine Schelde enters the modeled part of the system. The other boundary is near the North Sea.
The boundary data that are used are those collected for the SAWES model. Boundary conditions for the (transportable) state variables mesozooplankton, microzooplankton, ammonium, nitrate+nitrite, soluble silicate, chloride and oxygen were available as such.
Boundary conditions for the four phytoplankton groups were derived from boundary chlorophyll data, using carbon-to-chlorophyll ratios of adjacent compartments as calculated in the model and a forcing function expressing the fraction of diatoms which is present in the global algal pool. The latter really is undesirable, as one imposes to the model what one would like to see reproduced (i.e. a diatom bloom in spring followed by a flagellate bloom), but it was necessary to prevent either diatoms or flagellates from extinction. The same approach was adopted in SMOES.
The load of fast decay detritus at the boundaries is calculated from BOD (biochemical oxygen demand) values, using a conversion function as described in Thomann & Mueller (1987):
BODtoFDET = 1/((1-EXP(-BOD*5))*OCr)
where OCr is the amount (gram) of oxygen produced when mineralising 1 gram of carbon.
The load of slow decay detritus is calculated from boundary conditions of fast detritus by assuming that a fixed fraction of total detritus is slow decaying.

4.7 Waste loads

Waste loads were obtained from the SAWES model. Following substances (state variables) are imported through wastes: ammonium, nitrate+nitrite, dissolved silicate and detritus. Import of detritus is calculated from BOD values (see section 4.6).

5 Developing MOSES

5.1 Data gathering

Collecting data is one of the most difficult tasks in the modeling process. Yet it is an important one and the available data greatly determine the quality of the model. First a model requires data from laboratory and field experiments for underlying model assumptions on processes. Next physical data of the system, meteo data for forcing functions, data on discharges are needed. Calibration and validation are necessary to adjust and compare the model with reality.
For more information on the type of data gathered for the development of MOSES and their subsequent modification, we refer to addendum I.
The next step is to make a conceptual model in accordance with model aims. This concept includes a choice of state variables and processes to be formulated.
From these outlines of the model to the final program is only a relatively small step. This last step is supported by SENECA

5.2 Model structure

Based on the aims of the model and the available data, the model

developer has to structure the processes by giving names to one or more submodels, to choose the state variables, to formulate processes within the submodels in mathematical equations, decide which boundaries exist and which forcing functions, naming the process parameters and (intermediate) variables and give values to the parameters and starting values to the state variables. For a rationale about the choice of state variables, modeled processes, forcing functions and boundaries we refer to chapter 4.3, 4.4, 4.5 and 4.6.

The submodels which are defined In MOSES and the sequence in which they are called is represented in Figure 21.

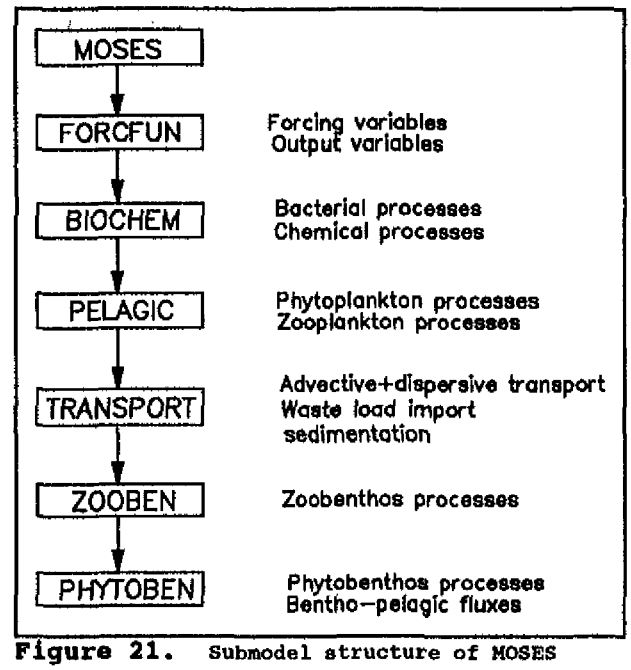

Figure 21. Submodel structure of MOSES

5.3 Parameterization

Ecological models are characterized by large uncertainties in their parameters. Carefully choosing the appropriate parameter values or ranges in a model can greatly determine the ultimate solutions and the speed with which these solutions are generated. In MOSES most parameter ranges were derived from SMOES (Klepper, 1989; Klepper et al., submitted) or from other relevant literature. The light-limitation function for phytoplankton primary production was patterned to Westerschelde light- and morphological characteristics by a parameterization of the formula of Klepper (1987, 1989) (see section 7.1, 7.1.2)

5.4 Calibration

The calibration of a complex ecosystem as this one is more an art than a science. All processes seem to be related in one way or another and it is rather difficult to assess what the effect of excluding some processes will be on the resulting model. However, it is impractical to implement the whole model at once and calibrate for the entire data set in one gigantic effort. Indeed, in developing the model one inevitably makes mistakes, which are relatively easy to find in a small submodel, but can be cunningly masked in a complex system. Moreover, as a first try, parameter ranges are kept as broad as possible (but without loosing their significance): we don't want to exclude some solutions at the very start ! Although biologically significant by itself, an extreme value of a parameter can produce impossibilities in combination with other parameters. Thus certain processes are bound to get stuck (as for instance concentrations become negative !) which makes the simulations very slow and many abortive runs can be expected.

The implementation strategy used in MOSES was thus to include submodels, keeping other processes which are esteemed to be significant as forcing functions. Calibration of this submodel then provides reduced parameter ranges which were used in the next calibration procedures. Although

appealingly simple, a major drawback is that a calibration can fine-tune a parameter range such that it compensates for the lack of some process. The consequent inclusion of this process will then find these parameter ranges unappropriate. If for instance the background mortality coefficient of some species is calibrated without the inclusion of its major predator, then this coefficient will be too high when the predator is included in the model. Nevertheless, to keep the implementation of this model manageable the successive implementation and calibration strategy was adopted. When we suspected that parameter ranges were too narrow, the nominal values were restored.

In short implementation and calibration proceeds as follows:

(1) Implementation and calibration of the transport model, modeling chlorinities (dissolved transport) and suspended load (particulate transport).
(2) Implementation of the pelagic submodel. Zooplankton biomass is at first kept as a forcing function but parameters which are important for the state variables in the submodel are included in the calibration.
(3) Full implementation of the zooplankton group. Hyperbenthos which predates on zooplankton is kept as a forcing function. Grazing rates of this group on zooplankton is included in the calibration.
(4) Inclusion of the benthos

5.5 Validation

The final step in the model excercise will be a validation. This will be achieved by running the model for two years which were not used in the calibration

6 Future developments and applications of MOSES

MOSES was built to investigate the origin and fate of organic carbon in the Scheldt estuary. The best summary for this kind of investigation is the annual integration of the carbon and nitrogen fluxes which are calculated by the model. As yet no such carbon or nitrogen budgets are included into MOSES. We believe this should be done at the very last instance when the calibration and validation has proven satisfactory. At the time of writing MOSES is still in its calibration stage.

The Scheldt estuary is one of the most polluted ecosystems throughout the world. Major problems are high concentrations of heavy metals and micro-organics (e.g. PCB's, PAC's). The behavior of these chemical species in the Westerschelde have been described in the model SAWES (SAWES, 1991). However no link to the animal food chain is provided in this model. Yet through this food web these pollutants can ultimately be incorporated into harvestable resources (fish or clams). Although MOSES is not intended to describe the behavior of this type of pollutants, modeling transport and incorporation of these pollutants in plants and animals could be instructive. How this has to be done, is beyond the scope of this report.

Developing an ecosystem model like MOSES can not be a goal in itself. One

wants to gain insight into the complexity of processes and interactions that take place in the system. At the time of writing this report the mathematical frame of MOSES was completed and the shaping of the model results to the observations has been started (calibration). However the latter process is rather time-consuming and it may be that some formulations are inadequate to describe the processes in the Westerschelde satisfactorily. This does not mean that the model has failed but it will indicate that the assumptions on which the model was based (and which incorporate our current understanding) have to be changed. One of these assumptions for instance is the food intake of the zooplankton. Some scientists believe that the zooplankton can discriminate algal food sources and reject other food if this resource is not limiting. Other scientists on the other hand state that indiscriminate feeding is the rule. In the Westerschelde it has been postulated that two modes of feeding are present: algal feeding in the mouth, indiscriminate feeding in the brackish part (Hummel et al., 1988). The findings of Soetaert & Van Rijswijk (submitted) show that there exists both a marine (allochtonous) and a brackish (autochtonous) community. However, recent expriments suggested that even brackish zooplankters selected for algae (Goosen, pers. comm). In MOSES only one mesozooplankton group has been defined which can either prefer algae or eat everything. If this scheme fails to reproduce zooplankton dynamics then it can be necessary to distinguish between a marine and a brackish zooplankton state variable, define a 'salinity stress' mortality coefficient as for phytoplankton and allow both groups to graze differently on phytoplankton and detritus.

Whereas scientists ask questions to the modeler like "why does.." or "Could it be that..", managers are more interested in "what.. if.." questions. For the Westerschelde such a question could be: "what would be the consequences for the ecosystem if Belgium would decrease its waste input by 50 %?" or "can the ecosystem stand a further increase of oxygen-demanding waste inputs" or "what would be the effect of increasing the suspended load by a factor X?". Undoubtedly a numerical model that integrates all kinds of processes into one functional unit is THE tool of answering such questions. Yet a healthy degree of skeptiscism is at its place. One should bear in mind that the model is developed to describe processes which were valid up till now and it has been shaped against past observations. If system states which are imposed to the model are very much different from the current states it could very well be that the model falls short and produces utter nonsense. This however is not a shortcoming of MOSES alone but of numerical models in general.

River nitrate concentration is affected by complex abiotic, biotic and anthropogenic factors and shows a marked relationship to population density (Peierls et al., 1991). This nitrate is transported to the coastal zone with sometimes undesirable consequences (blooms !). Recently there has been some controversy about the fate of nitrogen in the Scheldt estuary. Based on estimated in- and outputs of nitrogen, it has been postulated that a significant amount of nitrogen is eliminated from the estuary (about 75 10^3 kg of nitrogen per day) (Billen et al., 1985). Denitrification -in the sediment and in the near anoxic waters at the turbidity maximum- was indicated as the most important process for this nitrogen loss. This was confirmed by direct measurements which gave a denitrification rate in the watercolumn of up to .7 g N. m^{-3}. day^{-1} (Billen et al., 1985). Based on the model SAWES (1991) no such nitrogen loss was modeled in the Westerschelde (Van Eck et al., 1991). However, denitrification in SAWES is ignored in the sediment and is only allowed to occur in totally anaerobic

circumstances in the watercolumn (SAWES, 1988, 1991), whereas denitrification in the watercolumn is measurable from .2 g O_2 .m^{-3} and lower (Seitzinger, 1988). As totally anoxic conditions in the watercolumn rarely occur, denitrification cannot take place in SAWES. In sediments it has been shown that reduced microenviromnents in a generally aerobic layer can be the site of sulphate reduction (Jorgensen, 1977). As denitrification occurs at higher redox potentials than sulphate, this process can also be expected to occur. When the watercolumn has a high load of suspended organic matter as in the Westerschelde, rapid oxygen consumption by aerobic bacteria on the outside of detrital masses can also induce anoxic microenvironments where denitrification and sulphate reduction can occur (Caumette, pers. comm.). In MOSES an alternative implementation of the denitrification process (compared to SAWES) is built in: denitrification can occur in the -even aerobic- watercolumn, but is negatively influenced by higher oxygen conditions. Thus MOSES can be considered as an independent check on the validity of either one hypothesis.

7 A closer look at some processes and their implementation in MOSES

7.1 Light-limited primary production

7.1.1 The Eilers-Peeters model

The relationship between light intensity and the rate of photosynthesis in phytoplankton was described using the model of Eilers & Peeters (1988):

$$P=\frac{I}{aI^2+bI+c} \qquad \textbf{(1)}\ \text{Eilers \& Peeters (1988)}$$

with P the rate of photosynthetic production, I the light intensity and a,b,c characteristic parameters which determine the shape of the production-light intensity curve.
From this formula one can derive a dimensionless formulation:

$$\frac{P}{Pm}=\frac{(2+w)*u}{u^2+w*u+1} \qquad \textbf{(2)}\ \text{Eilers \& Peeters (1988)}$$

where $Pm=\frac{1}{b+2\sqrt{ac}}$, $w=\frac{b}{\sqrt{ac}}$, $u=\frac{I}{\sqrt{c/a}}=\frac{I}{I_{opt}}$,

Pm is the maximum primary production, Iopt is the light intensity where production is maximal. The parameter w (>=0) is a shape factor, determining the peakedness of the production curve: the lower w, the more pronounced is the potential photoinhibition.
Whereas w in the Eastern Scheldt varies between 0 and 15 (Klepper, 1989) the phytoplankton in the Westerschelde is characterized by a large degree of photoinhibition (data obtained from Kromkamp et al.): except for the wintermonths (w about 1), the shape factor is always zero indicating maximal inhibition (Figure 22.).

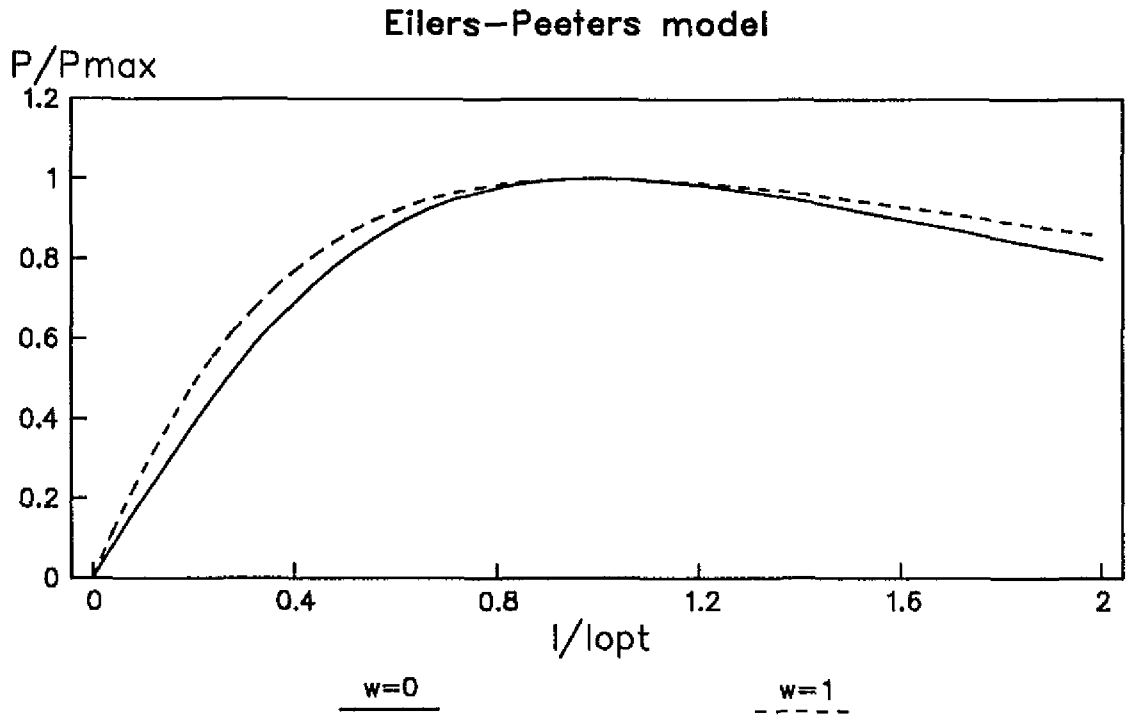

Figure 22.. Light-limitation function of Westerschelde populations.

7.1.2 Integrating over time and depth

In estuaries as well as in the sea, the quantity of light reaching the phytoplankton cells greatly depends on the depth of these cells in the water column whereas the light intensity also varies with the time of the day. Thus the formulae (1) or (2) should be integrated not only over the course of one day but also over depth. Moreover, to be applicable in field situations, the morphology of the Westerschelde needs to be taken into account: if a large fraction of the volume is concentrated in the deep tidal channels where light penetration is low, the average production per unit volume will be lower and vice versa.
In a global ecosystem model, integration of the photosynthetic formulae over time and depth is far too time-consuming and cumbersome. Thus the effect of decreasing light intensity with increasing depth into the water column, the effect of basin morphology and of fluctuating light intensity over a day was included into MOSES by fitting an equation of general form to depth averaged Westerschelde production as in Klepper (1987, 1989):

$$Lightlim = \frac{P}{Pmax * dl} = \frac{A*(1-e^{B*u})*(w+2)}{(k+C/depth)*(w+D)*depth} \qquad (3)\ \text{Klepper (1989)}$$

with Lightlim = a dimensionless reduction function, P = daily depth-averaged primary production, Pmax the maximal hourly primary production, dl the daylength in hours per day, u the average surface intensity expressed in units of Iopt (see formula (2)), w the factor describing the shape of the production curve (see formula (2)), k the extinction coefficient, depth the average depth (m) of the compartment and A,B,C and D coefficients which have to be fitted.

Klepper (1987, 1989) derived A,B,C and D of this model by independently varying the other parameters according to Eastern Scheldt characteristics and fitting the equation (3) through the calculated depth-integrated photosynthetic rates.
Instead, we used parameter values obtained from Kromkamp which describe real Westerschelde situations for 1991. The values of a,b and c in formula (1) were estimated based on incubator experiments, while the depth-integrated production was calculated for a completely mixed and stationary watercolumn using morphological data from SAWES (1991). This was done with the program written by Braat et al. (1990).
A nonlinear fit of formula (3) gave following estimates of A,B,C and D for the MOSES compartments:

MOSES nr	A	B	C	D
1	0.244	-1.32	1.29	6.51
2	0.185	-0.90	2.23	3.45
4	0.218	-1.04	-0.73	5.30
6	0.0933	-1.01	0.48	2.12
7	0.364	-0.90	0.31	7.92
9	0.305	-1.14	0.25	4.73
10	0.211	-1.23	2.72	5.10
11	0.222	-1.24	0.34	5.95
12	0.140	-1.27	0.13	3.84
13	0.193	-1.22	0.60	5.06

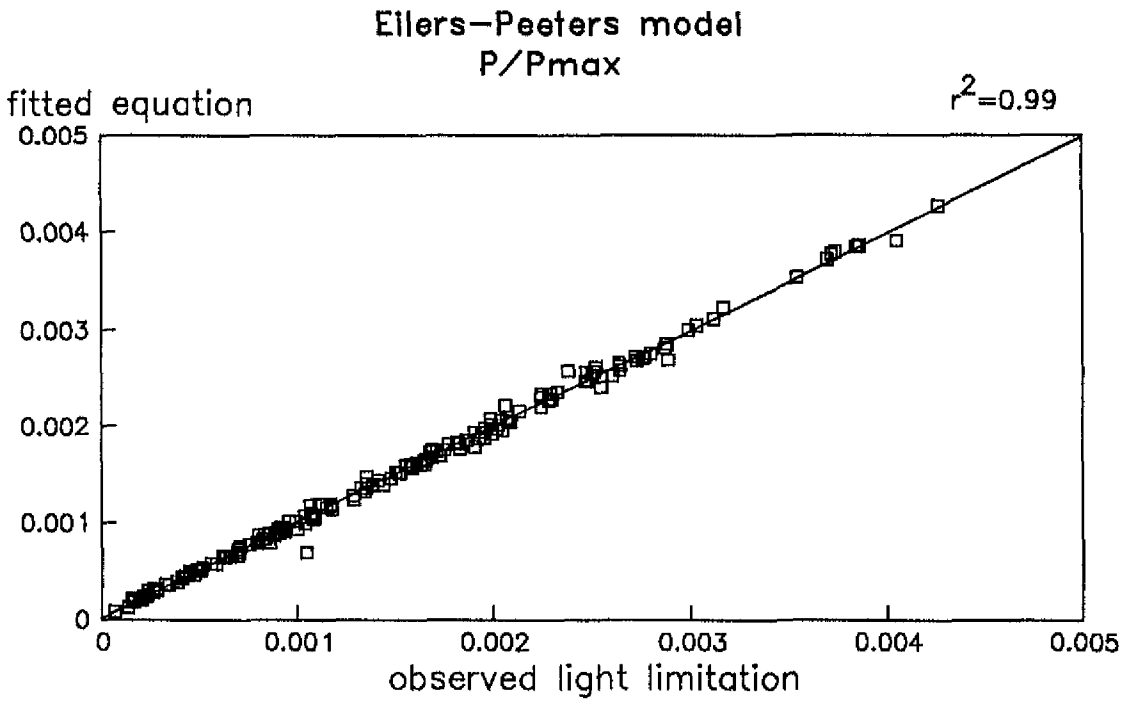

Figure 23.. Results of the Eilers-Peeters reduction formula.

The observed fit is given in Figure 23., while the light reduction as a function of light intensity for the compartments 1,7 and 9 is given in Figure 24..

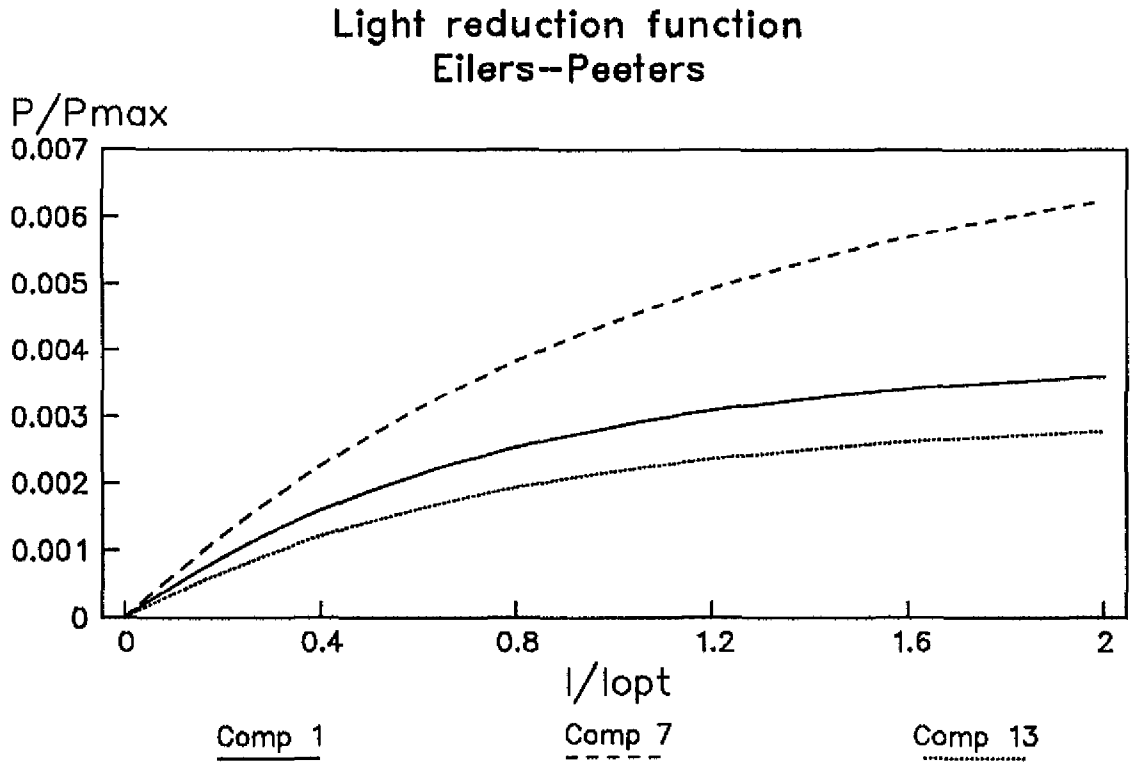

Figure 24.. Light reduction function for three MOSES compartments.

7.1.3 The effect of vertical mixing

Algal cells are not static and their vertical position in the watercolumn changes as a result of mixing. If the time-scale of light fluctuation due to mixing is much shorter than the time scale of adaptation of the algae, the resulting decrease in surface inhibition stands for an increase in depth-integrated production (Klepper et al., 1988). In the Scheldt estuary, tidal exchange is much higher than the freshwater flow (Van Eck et al., 1991) and vertical mixing is mainly tide-induced. In this case the degree of vertical mixing can be estimated as:

$$D_v = 0.0025 * Z * V_a \qquad \textbf{(4)}$$ Fisher et al.(1979)

with D_v the vertical dispersion coefficient in $m^2.s^{-1}$, V_a the depth-averaged amplitude of current velocity ($m.s^{-1}$) and Z the depth in meters. Using tidal current discharges in Bollebakker (1985) and cross surfaces and mean depth from SAWES (1991) a vertical dispersion coefficient of 52 $cm^2.s^{-1}$ at Vlissingen, decreasing to about 20 $cm^2.s^{-1}$ at Bath was calculated for the Westerschelde (compare with 100 to 400 $cm^2.s^{-1}$ in the Eastern Scheldt in Klepper et al., 1988). Based on a random walk model developed for the Eastern Scheldt (Klepper et al., 1988), these magnitudes of vertical dispersion stand for an increase in production of about 4 to 5 % for Easternscheldt conditions. Light attenuation in the Western Scheldt is much higher than in the Eastern Scheldt and thus the depth over which photoinhibition can occur is less in the latter, which will reduce the increase in production. On the other hand the algal populations show a larger degree of photoinhibition, which will make them more vulnerable to mixing effects. We expect that mixing will have a similar (negligible) effect on primary production as in Klepper et al. (1988). Moreover, in the Belgian part of the estuary where mixing is less pronounced, the effect of mixing should even be less. Therefore, this mixing factor was not taken into account in the model.

7.2 Benthic nitrogen and oxygen fluxes

As organic matter sediments to the bottom it is degraded by a sequence of oxidants. These reactions promote a flow of dissolved chemicals across the sediment-water interface (Malcolm & Stanley, 1982). Dynamical benthos models describing this degradation chain are complex and require a lot of computational power. Frequently one thus assumes that a steady state has been reached which allows the various fluxes and concentrations to be calculated in a more simple way. It has been shown that even extremely idealized diagenetic models can account for the major trends of the behavior of various substances in the sedimentary column (Billen, 1982).
From the Westerschelde only few (or no) data are available from chemical speciation in the bottom which makes the inclusion of a complex benthos model unwanted as it can not be calibrated. Moreover, a detailed description would necessitate the declaration of several new state variables which would further burden the speed of the model. It was thus decided to implement a model which calculates the fluxes of nitrogen species across the bottom-water interface without the necessity of modeling each benthic species separately.

7.2.1 Nitrogen flux

Diagenetic modeling consists in describing the vertical distribution of a given substance as a function of reaction, advection and mixing. The flux across the water-sediment interface can then be estimated by considering the vertical gradient at zero depth.
Based on this diagenetic modeling, an idealized model of nitrogen recycling was proposed by Lancelot & Billen (1985).
Here the rate of denitrification, and the release of nitrate and ammonia from the bottom is calculated from the input of organic matter to the bottom, from the overlying nitrate and oxygen concentration and from the mixing coefficient of the sediment interstitial and solid phases. The model distinguishes two degradable fractions C1 and C2 with first-order degradation constants k1 and k2 (day^{-1}) and Carbon to Nitrogen ratios CN1 resp. CN2. The input of this organic matter equals J1 resp. J2 (g $C.m^{-2}.day^{-1}$) Sediment bioturbation results in an apparent mixing coefficient Ds for the solid, Di for the interstitial phase ($m^2.day^{-1}$).
The model considers an oxic and an anoxic bottom layer. In the oxic layer organic matter is mineralized, thus producing ammonium. Nitrification (oxidation of ammonium) proceeds at a rate proportional to this aerobic degradation and is also restricted to the oxic layer. The anoxic layer is the site of denitrification (reduction of nitrate) which is defined as a first-rate process with respect to nitrate concentration.

The rate of organic matter degradation (g $C.m^{-3}.day^{-1}$) at sediment depth z is given by:

$$OMD(z) = J_1\sqrt{\frac{k_1}{D_s}}\exp^{\left(-\sqrt{\frac{k_1}{D_s}}z\right)} + J_2\sqrt{\frac{k_2}{D_s}}\exp^{\left(-\sqrt{\frac{k_2}{D_s}}z\right)}$$

(1) Lancelot & Billen (1985)

The maximum depth of oxygen penetration (Zn) in the sediment can be calculated by numeric solution of the following equation:

$$\frac{O_2^0 . D_i}{\alpha} - \frac{J_1}{\sqrt{\frac{k_1}{D_s}}} + \frac{J_2}{\sqrt{\frac{k_2}{D_1}}} + J_1 . \left(\frac{1}{\sqrt{\frac{k_1}{D_s}}} + z_n\right) \exp^{\left(-\sqrt{\frac{k_1}{D_s}} z_n\right)} +$$

$$+ J_2 . \left(\frac{1}{\sqrt{\frac{k_2}{D_s}}} + z_n\right) \exp^{\left(-\sqrt{\frac{k_2}{D_s}} z_n\right)} = 0$$

(2) Lancelot & Billen (1985)

with α the amount of oxygen respired for the aerobic mineralization of one amount of organic carbon.

The denitrification constant k_d (day^{-1}) is derived from the Michaelis-Menten half-saturation constant km (about 0.7 $g.m^{-3}$) in such a way that denitrification at the interface between oxic and anoxic layer is responsible for all organic matter degradation (at saturating nitrate concentration).

$$K_d = \frac{1}{2k_m} * NCrDenit * OMD(z_n)$$

(3) Lancelot & Billen (1985)

with NCrDenit the amount of nitrate reduced per amount of carbon degraded in the denitrification process.

Next the integrated rate of denitrification can be calculated as:

$$DENIT = -0.8 . \frac{J_1}{(C/N)_1} \exp^{\left(-\sqrt{\frac{k_1}{D_s}} zn\right)} - 0.8 . \frac{J_2}{(C/N)_2} \exp^{\left(-\sqrt{\frac{k_2}{D_s}} z\right)} - D_i A$$

(4) L & B (1985)

with

$$A = -\frac{1}{1 + Zn\sqrt{\frac{K_d}{D_i}}} . \left[\sqrt{\frac{K_d}{D_i}} . [A'] + 0.8 \frac{J_1}{D_i * (C/N)_1} \exp^{-\sqrt{\frac{k_1}{D_s}} z_n} +\right.$$

$$\left. + 0.8 \frac{J_2}{D_i * (C/N)_2} \exp^{-\sqrt{\frac{k_2}{D_s}} z_n}\right]$$

and

$$A' = C^0 + \frac{0.8 J_1}{D_i \sqrt{\frac{k_1}{D_s}} * (C/N)_1} . \left[1 - \exp^{\left(-\sqrt{\frac{k_1}{D_s}} z_n\right)}\right] +$$

$$+\frac{0.8J_2}{D_1\sqrt{\frac{k_2}{D_s}}*(C/N)_1}.[1-\exp^{(-\sqrt{\frac{k_2}{D_s}}z_n)}]$$

(remark the correction with respect to the formulation in Lancelot & Billen (1985).
Ultimately the fluxes of nitrate and ammonium across the sediment-water interface are:

$$F_{NO_3}=-0.8.\frac{J_1}{(C/N)_1}-0.8.\frac{J_2}{(C/N)_2}-D_1A$$

(5) L & B (1985)

and

$$F_{NH_4}=-\frac{J_1}{(C/N)_1}[1+0.8(\exp^{(-\sqrt{\frac{k_1}{D_s}}zn)}-1)]-\frac{J_2}{(C/N)_2}[1+0.8(\exp^{(-\sqrt{\frac{k_2}{D_s}}z_n)}-1)]$$

(6) L& B(1985)

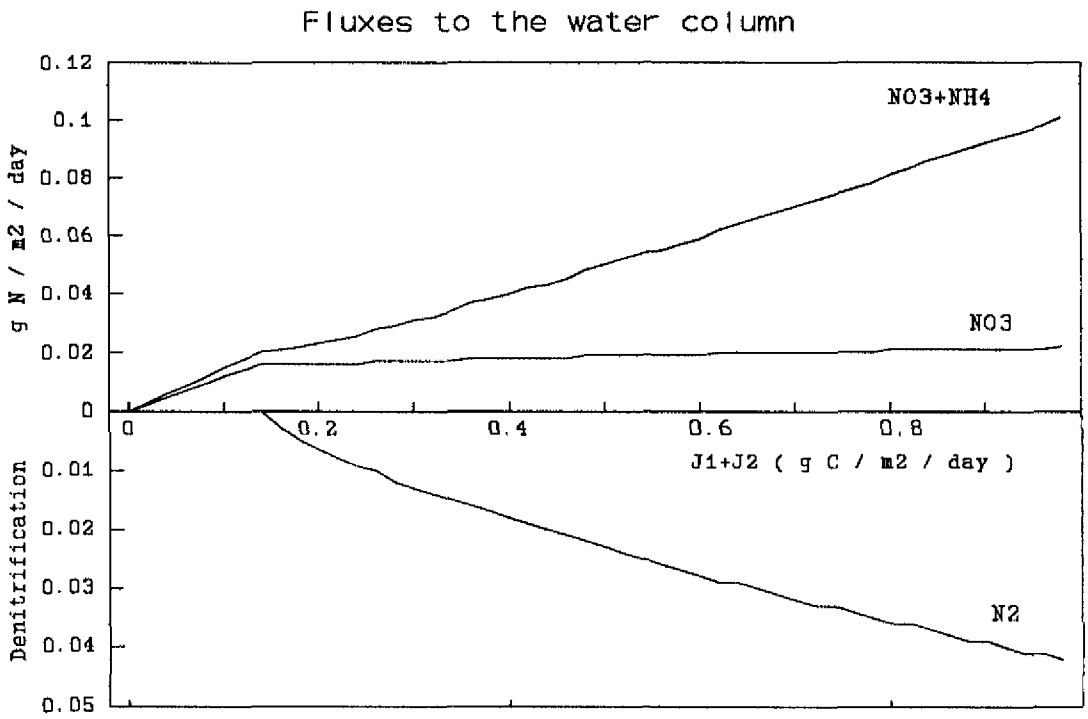

Figure 25. Nitrate and ammoniak fluxes from the bottom to the waterphase as a function of organic matter input.

One of the drawbacks of this kind of formulation is that the role of benthic fauna is not included. As bioturbators of the sediment they have an influence both on the mixing of the solid phase (reworking of the upper layers due to burrowing and feeding activities) and of the interstitial phase (pumping of invertebrates) (Billen, 1982). As it was not clear to what degree this benthic activity influences the value of the apparent mixing coefficient this was not included into MOSES.

7.2.2 Sediment oxygen demand

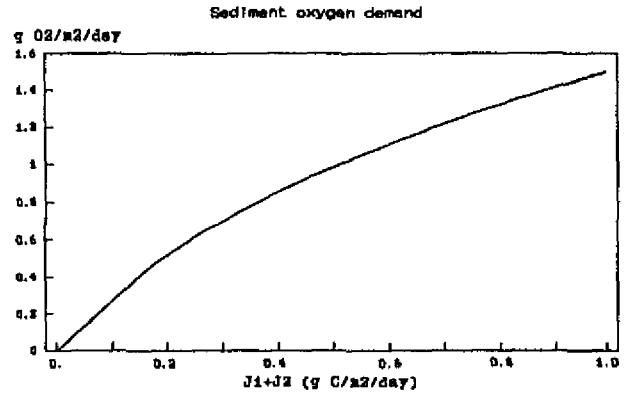

Figure 26. Oxygen flux from the water to the bottom.

The mineralisation of organic matter in the aerobic bottom layer and the nitrification requires a lot of oxygen which results in an oxygen flux from the overlying water to the bottom. This flux also has to be modeled in MOSES in a way that is consistent with the nitrogen budget as described in section 7.2.1. If advection due to sediment accumulation is ignored (as in the model of Lancelot & Billen, 1985) the flux of a dissolved species across the sediment-water interface is a function of the concentration gradient and the apparent diffusion coefficient of the interstitial water:

$$FluxO_2 = -D_1 * [\frac{dO_2}{dz}]_{z=0}$$

(7)Billen (1982)

The vertical distribution of oxygen is given by

$$\frac{dO_2}{dt} = 0 = D_1 \frac{d^2O_2}{dz^2} - \alpha [J_1 \sqrt{\frac{K_1}{D_s}} e^{-\sqrt{\frac{K_1}{D_s}} z} + J_2 \sqrt{\frac{K_2}{D_s}} e^{-\sqrt{\frac{K_2}{D_s}} z}]$$

(8) Lancelot & Billen (1985)

with boundary conditions

$$[\frac{dO_2}{dz}]_{(z=zn)} = 0$$

(9)Lancelot & Billen (1985)

it follows that

$$FluxO_2 = \alpha * [J_1 (1 - e^{-\sqrt{\frac{K_1}{D_s}} z_n}) + J_2 (1 - e^{-\sqrt{\frac{K_2}{D_s}} z_n})]$$

(10)

7.2.3 Calculating the load of organic carbon in the sediment

Although appealing that one can do without modelling each substance in the bottom, a major caveat of the diagenetic modeling is that higher organisms do consume benthic detritus (depositfeeders) and thus the detrital biomass which is available has to be known.
The concentration of organic matter C = C1+C2 at depth z can be calculated from the concentration at the bottom-water interface, the rate of decay and the apparent diffusion coefficient of the solid phase (if the same assumptions of the model of Lancelot & Billen, 1985) are valid:

$$C(z) = C_1(0)\exp^{(-\sqrt{\frac{k_1}{D_s}}z)} + C_2(0)\exp^{(-\sqrt{\frac{k_2}{D_s}}z)}$$

(11)Billen, 1982b

As

$$J_i = -D_s[\frac{dC_i}{dz}]_{(z=0)}$$

(12) Billen (1982b)

it follows that

$$C_i(0) = \frac{J_i}{D_s\sqrt{\frac{k_i}{D_s}}}$$

(13)Billen, 1982b

The mean concentration of organic matter in the sediment layer between depth x and y is

$$\overline{C_i} = \frac{1}{y-x}\int_x^y C_1(0)\exp^{-\sqrt{\frac{k_i}{D_s}}z}dz =$$

$$= \frac{J_i[\exp^{-\sqrt{\frac{k_i}{D_s}}x} - \exp^{-\sqrt{\frac{k_i}{D_s}}y}]}{(y-x)\,k_i}$$

(15)

with i indicating one of the degradable fractions (1 or 2).

7.2.4 Calculating the interstitial concentration of dissolved inorganic nitrogen species and oxygen

Although as yet no concentration profiles in the sediment have been measured, it is not unimaginable that this kind of data will eventually become available. Ideally we would like them to be incorporated into MOSES and use them as calibration data for the different fluxes.

The nitrate concentration at depth z is given by

$$C_{NO_3}(z) = .8\frac{J_1}{\frac{C}{N_1}\sqrt{\frac{k_1}{D_s}}D_i}[1-e^{-\sqrt{\frac{k_1}{D_s}}z}] + .8\frac{J_2}{\frac{C}{N_2}\sqrt{\frac{k_2}{D_s}}D_i}[1-e^{-\sqrt{\frac{k_2}{D_s}}z}] + Az + C_{NO_3}(0)$$

(16) Billen (1982b)

for z <= z_n, with A defined as above and

$$C_{NO_3}(z) = C_{NO_3}(z_n)\exp^{-\sqrt{\frac{k_d}{D_1}}(z-z_n)}$$

(17) Billen (1982b)

for z >= z_n.

Thus the concentration of nitrate in the sedimentlayer between depth x and y becomes:

$$\overline{C_{NO_3}} = \frac{1}{y-x}\int_x^y C_{NO_3}(z)\,dz =$$

$$= 0.8\frac{J_1}{\frac{C}{N_1}\sqrt{\frac{k_1}{D_s}}D_1} + 0.8\frac{D_s J_1}{\frac{C}{N_1}k_1(y-x)D_1}\cdot\left[e^{-\sqrt{\frac{k_1}{D_s}}y} - e^{-\sqrt{\frac{k_1}{D_s}}x}\right] +$$

$$+0.8\frac{J_2}{\frac{C}{N_2}\sqrt{\frac{k_2}{D_s}}D_1} + 0.8\frac{D_s J_2}{\frac{C}{N_2}k_2(y-x)D_1}\cdot\left[e^{-\sqrt{\frac{k_1}{D_s}}y} - e^{-\sqrt{\frac{k_2}{D_s}}x}\right] + \frac{A(y+x)}{2} + C_{NO_3}(0)$$

(20)

for z <= z_n and

$$\overline{C_{NO_3}} = \frac{1}{y-x}\int_x^y C_{NO_3}(z)\,dz =$$

$$= -\frac{C_{NO3}(z_n)}{(y-x)\sqrt{\frac{k_d}{D_1}}}\left[e^{-\sqrt{\frac{k_d}{D_1}}(y-z_n)} - e^{-\sqrt{\frac{k_d}{D_1}}(x-z_n)}\right]$$

(22)

for z >= z_n.

The ammonium concentration at depth z is given by

$$C_{NH_4}(z) = 0.2\frac{J_1}{(C/N)_1\sqrt{\frac{k_1}{D_s}}D_1}\left[1-\exp^{-\sqrt{\frac{k_1}{D_s}}z}\right] + 0.8\frac{J_1 z}{D_1(C/N)_1}\exp^{-\sqrt{\frac{k_1}{D_s}}z_n} +$$

$$+0.2\frac{J_2}{(C/N)_2\sqrt{\frac{k_2}{D_s}}D_1}\left[1-\exp^{-\sqrt{\frac{k_2}{D_s}}z}\right] + 0.8\frac{J_2 z}{D_1(C/N)_2}\exp^{-\sqrt{\frac{k_2}{D_s}}z_n}$$

(24)

(corrected from Billen, 1982b)

for z <= z_n and

$$C_{NH_4}(z) = C_{NH_4}(z_n) + \frac{J_1}{(C/N)_1\sqrt{\frac{k_1}{D_s}}D_f}\left[\exp^{-\sqrt{\frac{k_1}{D_s}}z_n} - \exp^{-\sqrt{\frac{k_1}{D_s}}z}\right] +$$

$$+ \frac{J_2}{(C/N)_2\sqrt{\frac{k_2}{D_s}}D_f}\left[\exp^{-\sqrt{\frac{k_2}{D_s}}z_n} - \exp^{-\sqrt{\frac{k_2}{D_s}}z}\right] \qquad (26)$$

for z >= z_n
(corrected from Billen, 1982b)

Thus the concentration of ammonia in the sedimentlayer between depth x and y becomes:

$$\overline{C_{NH_4}} = \frac{1}{(y-x)}\int_x^y C_{NH_4}(z)\,dz =$$

$$= .2\frac{J_1}{(C/N)_1\sqrt{\frac{k_1}{D_s}}D_f} + .2\frac{J_1 D_s}{(C/N)_1 k_1 D_f (y-x)}\left[e^{-\sqrt{\frac{k_1}{D_s}}y} - e^{-\sqrt{\frac{k_1}{D_s}}x}\right] + .8\frac{(y+x)\,J_1}{2D_f(C/N)_1}e^{-\sqrt{\frac{k_1}{D_s}}z_n} +$$

$$+ .2\frac{J_2}{(C/N)_2\sqrt{\frac{k_2}{D_s}}D_f} + .2\frac{J_2 D_s}{(C/N)_2 k_2 D_f (y-x)}\left[e^{-\sqrt{\frac{k_2}{D_s}}y} - e^{-\sqrt{\frac{k_2}{D_s}}x}\right] + .8\frac{(y+x)\,J_2}{2D_f(C/N)_2}e^{-\sqrt{\frac{k_2}{D_s}}z_n} \qquad (29)$$

for z <= z_n and

$$\overline{C_{NH_4}} = \frac{1}{y-x}\int_x^y C_{NH_4}(z)\,dz =$$

$$= C_{NH_4}(z_n) + \frac{J_1}{D_f(C/N)_1\sqrt{\frac{k_1}{D_s}}}e^{-\sqrt{\frac{k_1}{D_s}}z_n} + \frac{D_s J_1}{D_f(y-x)\,k_1(C/N)_1}\left[e^{-\sqrt{\frac{k_1}{D_s}}y} - e^{-\sqrt{\frac{k_1}{D_s}}x}\right] +$$

$$+ \frac{J_2}{D_f(C/N)_2\sqrt{\frac{k_2}{D_s}}}e^{-\sqrt{\frac{k_2}{D_s}}z_n} + J_2\frac{D_s}{D_f(y-x)\,k_2(C/N)_2}\left[e^{-\sqrt{\frac{k_2}{D_s}}y} - e^{-\sqrt{\frac{k_2}{D_s}}x}\right] \qquad (32)$$

for z >= z_n.

Similarly one can calculate the concentration of oxygen in sedimentlayers: solving equation (8) with boundary conditions

$O_2 = O_2(0)$ for $z = 0$;
$O_2 = dO_2/dz = 0$ for $z = z_n$;

gives

$$O_2(z) = -\frac{\alpha J_1 e^{-\sqrt{\frac{k_1}{D_s}}z}}{D_1\sqrt{\frac{k_1}{D_s}}} + \frac{\alpha z J_1 e^{-\sqrt{\frac{k_1}{D_s}}z_n}}{D_1} - \frac{\alpha J_1}{D_1\sqrt{\frac{k_1}{D_s}}} -$$

$$- \frac{\alpha J_2 e^{-\sqrt{\frac{k_2}{D_s}}z}}{D_1\sqrt{\frac{k_2}{D_s}}} + \frac{\alpha z J_2 e^{-\sqrt{\frac{k_2}{D_s}}z_n})}{D_1} - \frac{\alpha J_2}{D_1\sqrt{\frac{k_2}{D_s}}} + O_2(0) \qquad (34)$$

The oxygen concentration in a sediment layer from x to y is then

$$\overline{O_2} = \frac{1}{y-x}\int_x^y O_2(z)\,dz =$$

$$= -\frac{\alpha J_1 D_s}{D_1 k_1 (y-x)}\left(e^{-\sqrt{\frac{k_1}{D_s}}y} - e^{-\sqrt{\frac{k_1}{D_s}}x}\right) + \frac{\alpha (y+x) J_1}{2D_1} e^{-\sqrt{\frac{k_1}{D_s}}z_n} - \frac{\alpha J_1}{D_1\sqrt{\frac{k_1}{D_s}}} -$$

$$- \frac{\alpha J_2 D_s}{D_1 k_2 (y-x)}\left(e^{-\sqrt{\frac{k_2}{D_s}}y} - e^{-\sqrt{\frac{k_2}{D_s}}x}\right) + \frac{\alpha (y+x) J_2}{2D_1} e^{-\sqrt{\frac{k_2}{D_s}}z_n} - \frac{\alpha J_2}{D_1\sqrt{\frac{k_2}{D_s}}} + O_2(0) \qquad (37)$$

for $z <= z_n$
while the oxygen concentration is zero for a sediment layer deeper than z_n.

The fit between the concentration profiles as given in Billen (1982b) and the calculated concentrations in .5 cm sediment slices is given in Figure 27 to Figure 29.
These profiles and loads were calculated with subroutines that can be incorporated into MOSES.

7.2.5 Fitting the benthos into the diagenetic model

In MOSES we assume that the metazoan benthos does not behave differently from the microbes when the degradation of organic matter is considered: both the bacteria and the metazoa ultimately convert organic matter to CO_2 while producing ammonia. One could argue that the rate with which these processes occur is slower in metazoans, which could be translated into

lower decay coefficients of organic matter. However, their role is probably minimal compared to the microbial loop.
Similarly the food of benthic suspension feeders is added to the flux of organics to the sediment and it is assumed that the suspension feeders behave as the microbial loop. Dead benthic algae are also added to the net sedimentation flux.

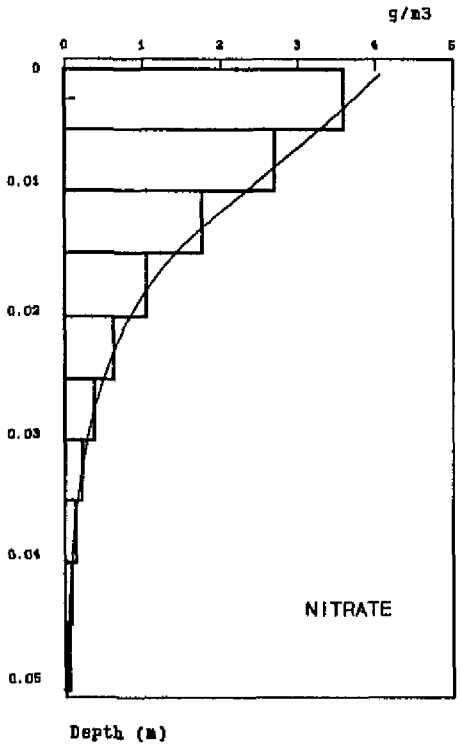

Figure 27 Nitrate profile in the sediment and calculated load according to the diagenetic model.

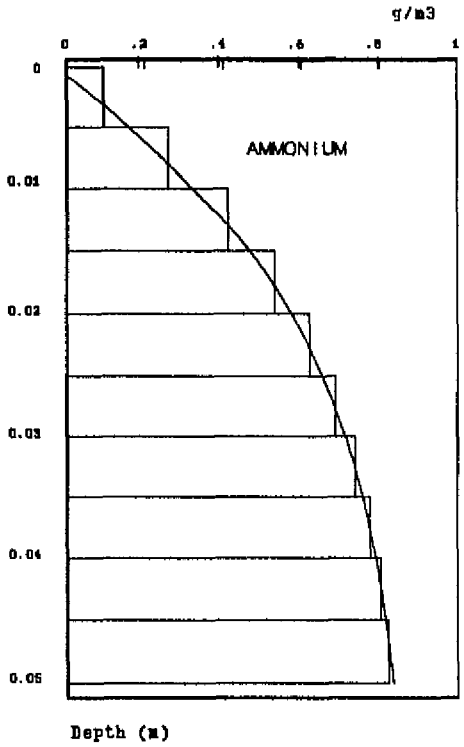

Figure 28 Ammonia profile in the sediment and calculated load according to the diagenetic model.

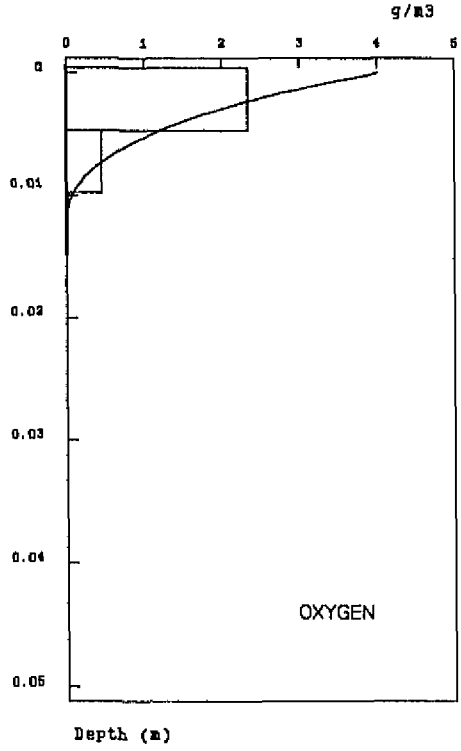

Figure 29 Oxygen profile in the sediment and calculated load according to the diagenetic model.

7.3 MOSES transport

7.3.1 Introduction

Estuaries are major pathways of organic and inorganic matter from land to sea and vice versa. Various chemical and biological processes in estuaries can profoundly change the speciation of nutrients and the composition of organic matter. Thus the residence time of substances in the estuary not only affects their transfer to the adjacent coastal zone but also determines their chemical and biological characteristics (Wollast, 1983). In order to thrive in the dynamic estuarine ecosystem, many organisms have life cycles with time scales that are comparable to the rate at which they are flushed to the sea. In order to be able to reproduce these various processes it is therefore important that a global ecosystem model of estuaries is based on an adequate description of transport processes.

7.3.2 Transport of dissolved substances

A dissolved substance in estuaries is transported seawards by means of the freshwater flow of the main stream and its tributaries (advective flow), while tidal forces induce short-term oscillatory movements, resulting in a strong mixing (Thomann & Mueller, 1987).

7.3.3 The dissolved transport equation

Mathematical models that follow the time and space distribution of a substance within a tidal cycle are complex, they need detailed information over one tidal cycle for calibration and require a long time for computer simulation. However, in ecological models with a time scale of years one is not interested in variations within a tidal cycle and the model equations can thus be simplified by considering the time scale to be composed of tidal cycle units (Thomann & Mueller, 1987). This is achieved by transposing the transport equation to a new reference frame, which oscillates with the tide so as to maintain a constant volume upstream. Further tidal oscillations are then removed by applying a time averaging operator (O'Kane, 1980). As such the complex partial differential equation describing mass transport within a tidal cycle is brought back to the much simpler differential equation which describes the concentration (s) of a substance as a function of time (t) and space (x):

$$\frac{\partial s}{\partial t} = -U\frac{\partial s}{\partial x} + E_x\frac{\partial^2 s}{\partial x^2} - Ks \qquad (1)$$

(Thomann & Mueller, 1987)
Mass transport is a function of the freshwater flow (advective transport, first term) and a transport caused by heterogeneities introduced by the tides (dispersive transport, second term). The third term of the equation is a reaction term.

Such differential equations can only in very general cases be solved analytically and one usually has to resort to approximate equations, which are solved numerically by computer. In practice one uses a 'finite difference' approximation of the equation. This means that one does not calculate the concentration at any position for any time, but one calculates values on a grid of points. Thus the estuary is subdivided into a series of segments, which are supposed to be homogeneous, i.e. there is no exchange within but only among segments. Only the average concentration in each segment can be estimated. In the case of the one-dimensional estuary the approximate spatial derivates for segment i give:

$$\frac{\partial s}{\partial x}\Big|_i = \frac{s_{i,i+1} - s_{i-1,i}}{\Delta x} \qquad (2)$$

The interfacial concentration $s_{i,i+1}$ (unknown) is related to the concentrations in segments i and i+1. Assuming the relationship is linear, one obtains $s_{i,i+1} = \alpha_{i,i+1}\, s_i + \beta_{i,i+1}\, s_{i+1}$, with $\alpha_{i,i+1} = 1 - \beta_{i,i+1}$; $0 <= \alpha <= 1$.

Ultimately, the differential equation (1) can be approximated by the following difference equation:

$$V_i \frac{\partial s_i}{\partial t} = Q_{i-1,i}(\alpha_{i-1,i} s_{i-1} + \beta_{i-1,i} s_i) - Q_{i,i+1}(\alpha_{i,i+1} s_i + \beta_{i,i+1} s_{i+1}) +$$

$$E^i_{i,i+1}(s_{i+1} - s_i) - E^i_{i-1,i}(s_i - s_{i-1}) - K_i s_i V_i \qquad (3)$$

with $E^i_{i,i+1} = E_{i,i+1} * A_{i,i+1} / \Delta x$,

$A_{i,i+1}$ being the flow interface between compartments,
Δx the dispersion length.

After approximating spatial changes, the temporal derivates which represent the time evolution are calculated. In SENECA, this is done in an explicit way, i.e. values at time t are calculated using values at the previous time step only. Implicit schemes use also information at the new time step.

7.3.4 Numerical errors

Approximating differential equations by difference equations introduces errors, and there are a number of criteria crucial to the ability of the numerical model to simulate transport processes correctly. Thus there exists the problem of computational instability, which implies an explosive growth of small errors, inevitably present in the numerical computations. Secondly, it can occur that some concentrations become negative. Thirdly, in addition to the true dispersion, an undesired 'dispersion' can be introduced (numerical dispersion). These errors put some restrictions on the possible values of the time and spatial step and of the weighing factor alpha:

Concentration positivity is ensured when

$$\alpha > 1 - \frac{E}{U\Delta x} \tag{5}$$

The stability criterion (for a 'constant coefficient estuary') is:

$$1 + U\frac{\Delta t}{\Delta x}(\beta - \alpha) - \frac{2E\Delta t}{\Delta x^2} - K\Delta t > 0 \tag{6}$$

Numerical dispersion is given by

$$E_{num} = U\Delta x[(\alpha - .5) - \frac{U\Delta t}{2\Delta x}] \tag{7}$$

In all types of error, the values of alpha (and beta) play part. Alpha was introduced in the equation as a weighing factor for estimating the concentration at the interfaces of segments. More specifically alpha indicates the importance of the upstream compartment. Thus, in a purely advective system, alpha should be one (i.e. a backward differencing scheme), while purely dispersive systems should have alpha set to 0 (or beta = 1, i.e. forward differences) (Thomann & Mueller, 1987). When using central differences, interfacial concentrations are mere averages of those of adjacing compartments.
With backward differences, positive concentrations are always ensured, but they introduce the largest numerical dispersion. Central differences can induce negative concentrations if the conditions in formula (4) are not met, but numerical dispersion caused by spatial differencing is zero when α is set to 0.5. There remains however an undesired dispersion caused by the forward explicit time differencing. In view of the general stability criterion (formula 5) it follows that the smaller alpha, the larger the time step can be.

The typical range of alpha in estuaries is .5<= alpha <= 1., with alpha being lower as the system becomes more dispersive (Thomann & Mueller, 1987). Many ecosystem models use the centered differencing scheme (Helder & Ruardy, 1982; Klepper, 1989).

Numerical instabilities put bounds on the time step, provided alpha and the spatial grid are fixed. In SENECA the implementation of the variable time step ensures that numerical errors remain within bounds, but as a result the simulation may become slow. It can be noted that implicit schemes are more efficient in handling this kind of error and it can be possible to use larger time steps. However, it could be that the implicit solution thus obtained, although it is stable, is not the real solution (Pond & Pickard, 1983).

7.3.5 Estimation of dispersion coefficients

The tidal dispersion coefficient E in equation (1) (or E' in equation 3) incorporates all effects which can not be ascribed to the freshwater flow in an estuary. As E generally cannot be calculated directly, it has to be estimated in some way. This is usually done by using a conservative substance (i.e. one that exhibits no decay) as a tracer if the advective flow is known. For estuaries the obvious choice of such a substance is

salinity.

Several estimation methods exist, based on different assumptions:

(1) In an estuary with a constant flow and a constant cross-sectional area, a crude estimate can be obtained by assuming there is no change in salinity with time. Solution of the equation (1) then gives (Thomann & Mueller, 1987; O'Connor et al., 1987):

$$E = \frac{Q_{i,i+1} * (x_{i+1} - x_i)}{A_{i,i+1} * \ln(s_{i+1}/s_i)} = \frac{Q * s}{A * ds/dx} \qquad (8)$$

with C_i the concentration at distance x_i.

(2) Dispersion coefficients can also be calculated by means of the 'fraction of freshwater' method (Thomann & Mueller, 1987). Here the dispersion across the most seaward boundary is calculated first. The other coefficients are then calculated working backwards and using previously calculated coefficients. This method is less restrictive than method (1) in that here physical characteristics of the estuary are taken into account. However, it is assumed that salinity does not change with time and that upstream mixing of the most upstream compartment is zero.

(3) Finally dispersion coefficients can be calculated by means of a calibration procedure, i.e., based on initial estimates those coefficients that best reproduce the observed salinity distribution are estimated iteratively.

Disadvantages of methods (1) and (2) are the uncertainties in the salinity profile. In (2) errors are propagated to the more upstream compartments. This requires that the data set should be smoothed carefully. Moreover, the obtained dispersion coefficients are valid only for the time instance at which the data set was procured. In order to be generally applicable, one needs to average somehow over the course of a year.
Although more time consuming, the calibration procedure (3) has the advantage of being less sensitive to measurement uncertainties. Moreover, a global coefficient is obtained as all salinity measures over the course of one or several years can be used. Finally, performing a calibration in SENECA is a piece of cake.

7.3.6 Implementation in MOSES

7.3.6.1 First try: an explicit scheme

In MOSES the general transport model (equation 3 in section 7.3.3) was implemented first in an explicit way. Tidal dispersion coefficients and the values of alpha were estimated by calibration on salinity profiles of 1982-1985 and using freshwater flows at the boundaries (method 3 in section 7.3.5). Initial estimates of E' were obtained from the SAWES model (SAWES, 1991). These estimates were obtained using method (1 in 7.3.5) and were based on chloride profiles of 1983 (SAWES, 1991).

Dispersion coefficients were at first calibrated using backward differences (i.e. $\alpha = 1$). This ensured absolute positive concentrations. Thus initial

estimates for the coefficients and reduced ranges were obtained. Based on these ranges and the maximal advective flows, the possible range for the alphas was calculated such as not to violate the positivity criterion (equation 4). In practice this implied that the value of α at the first two interfaces had to be 1, the third α had to be larger than .63. Other values could be within the range allowed: .5 - 1.
A second calibration both on the dispersive flows and the values of α was then run. As this did not result in a better GOF (.54 instead of .37), the first obtained values (backward differences) were retained.

7.3.6.2 Increasing the speed: implicit scheme

As noted before, explicit schemes as the one used this far can suffer from computational instabilities (formula 5). In order to avoid instabilities in the SAWES compartments 6 and 7 (Van Eck, personal communication), these two were already combined into one MOSES 5 compartment. However, now instabilities in the compartments 7 and 8 were determining the small time step chosen by the integration routine in SENECA. As the time step became inbearably slow, and as incorporation of a reactivity term further increases this phenomenon, it was decided to implement an implicit transport submodel instead of the explicit one above.
Whereas in an explicit scheme one only uses data of the previous time step to calculate derivates at the current time step, a fully implicit scheme uses data only at the current time step. Thus with α set to 1

$$V_i * \frac{(s_i^{t+\Delta t} - s_i^t)}{\Delta t} = Q_{i-1,i} s_{i-1}^{t+\Delta t} - Q_{i,i+1} s_i^{t+\Delta t} +$$

$$E'_{i,i+1}(s_{i+1}^{t+\Delta t} - s_i^{t+\Delta t}) - E'_{i-1,i}(s_i^{t+\Delta t} - s_{i-1}^{t+\Delta t})$$

with S_i^t = concentration in compartment i at time step t.

Rearranging one obtains:

$$s_i^t = \frac{\Delta t}{V_i} * [-(Q_{i-1,i} + E'_{i-1,i}) s_{i-1}^{t+\Delta t} + (\frac{V_i}{\Delta t} + Q_{i,i+1} + E'_{i,i+1} + E'_{i-1,i}) * s_i^{t+\Delta t} - E'_{i,i+1} s_{i+1}^{t+\Delta t}]$$

and at the boundaries:

$$s_1^t = \frac{\Delta t}{V_1} * [-(Q_{0,1} + E'_{0,1}) s_0^{t+\Delta t} + (\frac{V_1}{\Delta t} + Q_{1,2} + E'_{1,2} + E'_{0,1}) * s_1^{t+\Delta t} - E'_{1,2} s_2^{t+\Delta t}]$$

and

$$s_{13}^t = \frac{\Delta t}{V_{13}} * [-(Q_{12,13} + E'_{12,13}) s_{12}^{t+\Delta t} + (\frac{V_{13}}{\Delta t} + Q_{13,sea} + E'_{13,sea} + E'_{12,13}) * s_{13}^{t+\Delta t} - E'_{13,sea} s_{sea}^{t+\Delta t}]$$

Or, in matrix formulation and putting $E'_{0,1} = 0$ (no dispersion at the upper boundary):

$$\begin{vmatrix} b_1 & c_1 & 0 & 0 & 0 \\ a_2 & b_2 & c_2 & & \\ 0 & a_3 & b_3 & c_3 & \\ \cdot & & & & \\ \cdot & & & & \\ 0 & 0 & 0 & a_{13} & b_{13} \end{vmatrix} * \begin{vmatrix} s_1^{t+\Delta t} \\ s_2^{t+\Delta t} \\ s_3^{t+\Delta t} \\ \cdot \\ \cdot \\ s_{13}^{t+\Delta t} \end{vmatrix} = \begin{vmatrix} s_1^t + \Delta t/V_1 * Q_{0,1} * s_0^{t+\Delta t} \\ s_2^t \\ s_3^t \\ \cdot \\ \cdot \\ s_{13}^t + \Delta t/V_{13} * E'_{13,sea} * s_{sea}^{t+\Delta t} \end{vmatrix}$$

(9)

with $a_i = -\Delta t/V_i \ (Q_{i-1,i} + E'_{i-1,i})$

$b_i = 1+\Delta t/V_i \ (Q_{i,i+1} + E'_{i-1,i} + E'_{i,i+1})$

$c_i = -\Delta t/V_i * E'_{i,i+1}$

As the terms $s_{sea}^{t+\Delta t}$ and $s_0^{t+\Delta t}$ on the right hand side are to be calculated on the next time step, they are substituted by the explicit terms s_{sea}^t and s_0^t .

Thus the transport submodel reduces to the solution of a tridiagonal set of linear algebraic equations, which can easily be solved for all $s_i^{t+\Delta t}$ by backsubstitution (Press et al., 1987).

This method was implemented in the MOSES tranport submodel as follows: for every compartment i the concentration at time step t+1 (i.e. one SENECA time unit later) was estimated by solving equation (9) with Δt set to 1. The temporal derivates were then calculated as:

$$\frac{ds_i}{dt} = s_i^{t+1} - s_i^t$$

and submitted to the integration routine of SENECA.
The dispersion coefficients already obtained by the explicit method were further improved by calibration. The results are given in pages 60 to 62.

The speed of including this implicit transport submodel into MOSES increased substantially (10 to 100 times): 10 days simulation of MOSES required only 15 time steps in the implicit, 913 time steps in the explicit scheme !. Moreover, chloride concentrations as predicted by the implicit model, were highly comparable to the ones obtained by the explicit scheme (figure).

Although the implicit scheme may fail to converge to the real solution if time steps are taken too large (Pond & Pickard, 1989), the gained speed and probably negligible loss of accuracy strongly advises to use the implicit method. Moreover, the integration routine in SENECA still guards against too large time steps.

7.3.7 Horizontal transport of particulate matter

Whereas the net flow of dissolved material is function of the freshwater discharge in the estuary, particulate matter transport can be entirely independent and even opposite to this seaward transport. Reasons are the asymetry in tidal velocities during the eb and flood phase resulting in more erosion during flood, the fact that resuspension of particles requires higher velocities than sedimentation and, in partially mixed estuaries, the existence of a landinward current near the bottom (Postma, 1967; Dronkers, 1986; Dyer, 1988).

7.3.8 One-dimensional mud transport

Although depth-integrated, one-dimensional models are barely fit to simulate mud transport in estuaries (Odd, 1988), it is beyond the scope of MOSES to implement a multi-dimensional transport model. In the Westerschelde estuary, particulate transport is further complicated by intense dredging activity (Belmans, 1988).
For the current model, particulate transport is modelled as in Klepper (1989). In contrast with dissolved matter transport, particles are moved in the model by means of an 'apparent or particulate flow':

$$Ta = Q' * C.$$

with Ta = residual transport of suspended sediment ($g.s^{-1}$), Q' = apparent (or particulate) flow (in $m^3.s^{-1}$) and C the suspended sediment concentration ($g.m^{-3}$).
Apart from the residual transport, a degree of mixing similar to dispersion of dissolved substances occurs, which can be described with the same dispersion coefficients as determined for dissolved substances (Klepper, 1989).

7.3.9 Implementation in MOSES

The total particulate flow was at first calculated from quarterly net transport values for marine and fluviatile silt obtained from the SAWES model (SAWES, 1991). These net transport values were also used to estimate net sedimentation rates: on the long run there has to be an equilibrium between what comes into a compartment and what goes out, differences are either due to resuspension or sedimentation.
A first approximation of the particulate flow was done as follows: total net transport was divided by mean concentration of particulate matter and the dispersive flux (obtained from dissolved transport) was substracted (see Klepper, 1989). Next the thus obtained 'apparent flows' were used as initial values in a calibration procedure. Suspended matter (corrected for organic matter) was allowed to change due to import across the boundaries (sea, freshwater), due to waste loads and net sedimentation and was transported with a model as described in section 7.3.8. A calibration on the apparent particulate flow was run, using the load of suspended matter (SAWES data set) as observed data. In order to be consistent, we used the

latter transport values in MOSES.
As in MOSES the particulate load is calculated rather than using observed data (due to the erratic nature of this data set), a second calibration was run on these calculated values.
Values of the particulate flux thus obtained are in table (2) and the produced GOF in figures (2 and 3).
Remark the large degree of scatter in the observed data of suspended matter. This is due to the variable time of sampling with respect to the phase of the tide. The standardization of the data set did include a correction for the sampling position (i.e. the sampling is transposed to the position at slack tide) but concentration differences due to the variable current speed at different phases of the tide were not accounted for.

MOSES does not pretend to model mud transport in an exhaustive way. The main interest in modeling the transport of particulate substances is to obtain a transport equation for phytoplankton, zooplankton and detritus. As these have a vertical distribution somewhat inbetween those of dissolved and particulate matter, it is assumed that their transport behavior is also inbetween both. Thus they are attributed a parameter p, indicating their 'dissolved like behavior' and the net (advective) flow Q can then be calculated as

$$Q = Q'.(1-p) + p.Qadv$$

with Q' the (apparent) particulate flow, Qadv the advective (freshwater) flow (Klepper, 1989). An additional dispersive flow term (equal to the dissolved transport) models mixing.

The load of suspended matter is an important factor in the ecosystem as it determines the penetration of light in the water column. As it is not modeled in MOSES, it is calculated as a function of freshwater flow and position along the estuary.

7.3.10 Resuspension and sedimentation

No data on resuspension and sedimentation are available. Yet knowledge of the input of organic matter to the bottom is important for the calculation of the nitrogen- and oxygen exchange between bottom and watercolumn (see also section 7.2).
The bottom morphology distinguishes between the intertidal, subtidal and the (inert) gullies.
It was assumed that in the intertidal area a constant fraction of organic matter sediments. This fraction was calibrated in the ecological model.
The subtidal area is subject to a net sedimentation which was derived from Van Maldegem et al. (1991), (figure 7: 'natural' net sedimentation, figure 6: 'averaged mud content'). These net sedimentation values are represented in table 3.
Some compartments represent sources of silt (erosion or wastes), others are sinks. Erosion mainly takes place in compartments 2 and 4, while deposition is most pronounced in MOSES compartments 12 and 8.

Based on these net sedimentation rates ($g/m^2/(g/m^3)/day$) it is desirable to estimate sedimentation and resuspension rates (day^{-1}). Although the model is tide-averaged, we do want to include the effects of the tide in some way (for horizontal transport this was done by introducing a degree of mixing or dispersion). Thus, whereas there may be a net sedimentation or

resuspension in a compartment, a considerable amount of sediment is resuspended at high tidal velocities and settles when currents speed down. Thus there is an appreciable exchange of matter between the bottom and the water column we would like to incorporate into the model.

A simulation was run to calculate total sedimentation and resuspension rates.
Net sedimentation (NS) in compartment I can be represented as:

$$NS(I) = a(I)*Cw(I) - b(I)*Cb(I)$$

with a = sedimentation rate (time-1), Cw = concentration of 'mud' in the water, b = resuspension rate (time-1) and Cb = concentration of 'mud' in the bottom. NS is known, a and b have to be calibrated. As this results in too few equations in too many unknowns, the resuspension rate was assumed to be inversely related to sedimentation rate: $b(I) = K/a(I)$; with K a constant, equal for all compartments. Thus:

$$NS(I) = a(I)*Cw(I) - K/a(I)*Cb(I)$$

Data to calibrate against are: quarterly net sedimentation rates per compartment and a time series of suspended matter per compartment.

However, the results up till now are very unsatisfactory and it was decided not to proceed with this.

8 General remarks

Part of this modeling exercise was to be a test of the modeling package SENECA as developed by Scholten et al. (1989). In view of the short time span in which this ecosystem model has been developed (start in november 1991 - end in march 1992), using this programming tool for the implementation of a (complex) ecosystem model as MOSES seems to have been very valuable. Not only is the model developer relieved from implementation of numerical integration, calibration and sensitivity analysis, the user-friendly interface allows for rapid implementation of each submodel. Moreover a quick look on the output of each simulation is easy due to the extensive graphical possibilities. As calibration proved to be the speed-limiting factor of the development, at a certain time TWO models were present: one which was used for calibration and another -more complete one- where other process descriptions were added. Adding a submodel from one model to the other was not a problem in SENECA.

Some routine jobs however still proved to be somewhat cumbersome: initialising state variables and large parameter arrays requires a lot of <enter>ing and cursor use. Maybe some kind of 'import' routine could be added.

When it was decided to uncouple the bottom and pelagic compartments, it became clear that introducing more than thirteen bottom compartments would require a corresponding increase in the number of pelagic state variables as in SENECA state variables are automatically defined in each compartment. Fortunately we could do with thirteen bottom compartments. Nevertheless it could be desirable to uncouple the number of compartments and state variables.

The model was developed on a olivetti M380 computer with a 386 (25 MHz) processor and a 387 coprocessor. For just one run this machine proved to be fine but calibration was a timely business and proved to be the time limiting factor in model development. Whenever available, calibration was run on a 486 computer with coprocessor.

9 Summary

By order of Rijkswaterstaat, the Netherlands, an ecosystem model was developed for the Westerschelde, called MOSES.
MOSES (MOdel of the Scheldt EStuary) provides a mathematical frame for biological and biochemical processes which are deemed to be important in the Scheldt estuary. It ultimately should provide us with more insight into the functioning of this complex ecosystem.

Modelers tend to have a simplified perception of an ecosystem and in the case of MOSES our caricature of the Scheldt can be summarized as follows.
In the turbid waters of the Scheldt estuary, phytoplankton primary production is mainly light-limited. The algae consume nitrate and -preferentially- ammonia as a source of nitrogen, while diatoms also need

dissolved silicate for incorporation into their skeletons (frustules).
The algae consist of fresh-water and brackish-marine species and are grazed upon by the zooplankton (meso- and micro-), by the hyperbenthos and by the benthic filterfeeders. The hyperbenthos also consumes large amounts of zooplankton. Animals convert organic matter into carbon dioxide, detritus and ammonia while consuming oxygen.
The estuary is characterized by a large input of detrital carbon. This detritus is attacked and converted into bacterial biomass using oxygen or -in more anaerobic conditions- nitrate as an oxidans (denitrification). This mineralisation process causes a -near to- depletion of oxygen near the turbidity maximum.
The pelagic detritus -and associated bacteria- provides food for the zooplankton, hyperbenthos and benthic filterfeeders.
Benthic primary production is restricted to the intertidal flats. The zoobenthos also has highest biomasses in this region. They are filterfeeders (which capture food from the pelagic realm) or depositfeeders; the latter group feeds on benthic diatoms and sedimented detritus.
Important (bio)chemical reactions are the oxidation of ammonia to nitrate and the dissolution of particulate silicate.
Organic matter which sediments to the bottom is degraded by a sequence of oxydants, first oxygen, then nitrate. In the aerobic sediment zone, ammonia is oxydized to nitrate. These reactions promote a flux of oxygen from the water to the bottom, while ammonia and -in most cases- nitrate are released from the bottom to the water column.

While developing the model, model descriptions were kept as simple as possible. The mathematical formulation was mainly based on the formulation of the Eastern Scheldt model (SMOES, Klepper, 1989). In contrast with SMOES, MOSES distinguishes two dissolved nitrogen species while the benthic fluxes have been described based on diagenetic modeling. MOSES also shows higher spatial resolution than SMOES: averse to all superstition, thirteen pelagic and thirteen benthic compartments were discriminated. Benthic intertidal compartments are morphologically distinct units rather than associated with a pelagic compartment.

A global ecosystem model like MOSES is never finished and should profit from a cooperation between "scientists in the field" and modelers. As new insights into specialized disciplines become available they ought to be incorporated into the model and thus provide us with a more precise view of the real world.

Finally one could hope that a simulation package like SENECA will close the gap between modelers, i.e. "those who never wet their boots" and field scientists, i.e. "those who never have seen differential equations without a strong feeling of nausea".

10 Addenda

I: Data gathering and data modification for the development of MOSES.

11 Acknowledgements

The authors wish to thank G.Th.M. van Eck, project manager of the SAWES project of Rijkswaterstaat, who allowed us to use data, collected and worked up for SAWES. A. Schouwenaar is thanked for his efforts to pick out the data we wanted from a large data base.

Other people who delivered data, used in the MOSES data base, are: J. Craeymeersch (CEMO), V. Escaravage (CEMO), J. Kromkamp (CEMO), J.Mees (R.U.G.), J. Peene (CEMO), A. Van Spaendonk (CEMO), W. de Winter (CEMO).

Thanks are also due to Ir. I. Coen of het Ministerie van de Vlaamse Gemeenschap, Dienst Hydrologie and Ir. H. Belmans of de 'Antwerpse Zeehavendiensten, Loodsgebouw for providing us with data on Basin morphology of the Belgian part of the Scheldt.

Special thanks also to drs. John Schobben (project manager at the Tidal Water Division of Rijkswaterstaat), drs. Marcel van der Tol and Richard Duin who gave critical comments on this report.

The efforts to build this model are paid by the Rijkswaterstaat, Tidal Waters Division, within the project ECOLMOD-SIM, contract-number DGW-911G. This is the project in which SENECA was developed.

12 References

Baretta, J. & P. Ruardij, 1988. Tidal flat estuaries. Simulation and analysis of the Ems estuary. Springer-Verlag, Berlin.

Belmans, H., 1988. Verdiepings- en onderhoudsbaggerwerken in wester- en zeeschelde. Water 43 (1): 184-194.

Billen, G., 1975. Nitrification in the Scheldt Estuary (Belgium and the Netherlands). Estuar. Coast. Mar. Sci. 3: 79-89.

Billen, G., 1982. Modelling the processes of organic matter degradation and nutrient recycling in sedimentary systems. In D.B. Nedwell & C.M. Brown (Eds), 'Sediment microbiology' pp. 15-52. Academic Press, New York.

Billen, G., 1982b. An idealized model of nitrogen recycling in marine sediments. American Journal of Science 282: 512-541.

Billen, G., M. Somville, E. de Becker & P. Servais. 1985. A nitrogen budget of the Scheldt hydrographical basin. Neth. J. Sea Res. 19(34): 223-230.

Billen, G., C. Lancelot, E. De Becker & P. Servais, 1986. The terrestrial marine interface: modelling nitrogen transformations during its transfer through the Scheldt river system and its estuarine wone. In Nihoul, J.C.J. (ed.) Marine interfaces Ecohydrodynamics: 429-490. Elsevier.

Billen, G. & C. Lancelot, 1988. Modelling benthic nitrogen cycling in temperate coastal ecosystems. In: Blackburn, T.H. & J. Sorensen (eds.). Nitrogen cycling in coastal marine environments. SCOPE. John Wiley & Sons, Chichester: 341-378.

Braat, M.P.W.J., R.N.M. Duin & P.M.J. Herman, 1990. Primaire produktie programma. versie 1.03. Rapport DIHO 1990-08. Delta Instituut voor Hydrobiologisch onderzoek, Yerseke.

Bollebakker, G.P., 1985. Ijking en verificatie van het een-dimensionaal mathematisch model IMPLIC voor het scheldebekken met bodemligging 1981. Nota WWKZ-85.v006.

de Hoop, B.J., P.M.J. Herman, H. Scholten & K. Soetaert, 1992. SENECA 1.5. A Simulation ENvironment for ECological Application. MANUAL

Di Toro, D.M., D.J. O'Connor & R.V. Thomann, 1971. A dynamic model of the phytoplankton in the Sacramento-San Joaquin Delta. Adv. Chem. Series 106: 131-150.

Dronkers, J., 1986. Tide-induced residual transport of fine marine sediment. In: J van de Kreeke (ed.) Physics of shallow estuaries and bays. Springer lecture notes on coastal and estuarine studies 16, Berlin.

Duursma, E.K., A.G.A. Merks & J. Nieuwenhuize. 1988. Exchange processes in

estuaries as the Westerschelde, an overview. Hydrobiological Bulletin 22(1): 7-20.

Dyer, K.R., 1988. Fine sediment transport in estuaries. In: Dronkers, D. & van Leussen, W. (eds) Physical processes in estuaries. Springer-Verlag, Berlin. 295-310.

Eilers, P.H.C. & J.C.H. Peeters, 1988. A model for the relationship between light intensity and the rate of photosynthesis in phytoplankton. Ecol. Modell. 42: 185-198.

Eppley, R.W., 1972. Temperature and phytoplankton growth in the sea. Fish. Bull. 70: 1063-1085.

Fenchel, T., 1982. Ecology of heterotrophic microflagellates. IV. Quantitative occurrence and importance as consumers of bacteria. Mar. Ecol. Progr. Ser. 9: 35-42.

Fisher, H.B., E.J. List, .C.Y. Joh, J. Imberger & N.H. Brooks (1979). Mixing in coastal and inland waters. Acad press, New York.

Garber, J.M., 1984. Laboratory study of nitrogen and phosphorus remineralization during the decomposition of coastal plankton and seston. Est. Coast. Shelf Sci. 18: 685-702.

Heip, C., 1988. Biota and abiotic environment in the Westerschelde estuary. Hydrobiological Bulletin 22(1): 31-34.

Heip, C., 1989. The ecology of the estuaries of Rhine, Meuse and Scheldt in the Netherlands. In: J.D. Ros (Ed.) Topics in marine biology. Paper presented at the 22th European Marine Biology Symposium in Barcelona, Spain.

Helder, W. & P. Ruardij, 1982. A one-dimensional mixing and flushing model of the Ems-Dollart estuary: calculation of time scales at different river discharges. Neth. Journ. Sea Res. 15: 293-312.

Herman, P.M.J., H. Hummel, M. Bokhorst & A.G.A. Merks, 1991. The Westerschelde: interaction between eutrophication and chemical pollution? In: M. Elliott & J.-P. Ducrotoy (Eds.): Estuaries and coasts: spatial and temporal inercomparisons, ECSA19 Symposium, Olsen & Olsen.

Hummel, H., G. Moerland & C. Bakker. 1988. The concomitant existence of a typical coastal and a detritus food chain in the Westerschelde estuary. Hydrobiological Bulletin 22(1): 35-41.

Jorgensen, B.B., 1977. Bacterial sulphate reduction within reduced microniches of oxidized marine sediments. Marine Biology 41: 7-17.

Klepper, O., 1987. Fytoplanktonmodule Westerschelde. GWWS 87.204.

Klepper, O. & J. Stronkhorst. 1988. Steady state model of carbon flows in the Western Scheldt ecosystem. Notitie GWWS.89.621, DGW, The Hague, Middelburg.

Klepper, O., J.C.H. Peeters, J.P.G. van de Kamer & P. Eilers, 1988. The calculation of primary production in an estuary. A model that

incorporates the dynamic response of algae, vertical mixing and basin morphology. In: Marani, A. (ed): Advances in environmental modelling, Elsevier: 373-394.

Klepper, O, 1989. A Model of Carbon Flows in Relation to Macrobenthic Food Supply in the Oosterschelde Estuary (S.W. Netherlands). Ph. D. thesis, University of Wageningen, Wageningen, 1-270.

Klepper, O., M.W.M. Van der Tol, H. Scholten & P.M.J. Herman, (submitted) SMOES a simulation model for the oosterschelde ecosystem. Part I: description and uncertainty analysis.

Kremer, J.N. & S.W. Nixon, 1978. A coastal marine ecosystem. Simulation and analysis. Springer Verlag, Berlin.

Lancelot, C. & G. Billen, 1985. Carbon-nitrogen relationships in nutrient metabolism of coastal marine ecosystems. Adv. Aquat. Microbiol. 3: 263-321.

Linley, E.A.S., R.C. Newell & M.I. Lucas, 1983. Quantitative relationships between phytoplankton, bacteria and heterotrophic microflagellates in shelf waters. Mar. Ecol. Progr. Ser. 12: 77-89.

Malcolm, S.J. & S.O. Stanley, 1982. The sediment environment. In D.B. Nedwell & C.M. Brown (Eds), 'Sediment microbiology' pp. 15-52. Academic Press, New York.

McCarthy, J.J., W.R. Taylor & J.L. Taft, 1977. Nitrogenous nutrition of the plankton in the Chesapeake Bay. 1. Nutrient availability and phytoplankton preferences. Limnol. & Oceanogr. 22: 996-1011.

Mees, J. & O. Hamerlynck, submitted. Spatial community structure of the permanent hyperbenthos of the Schelde-estuary and the adjacent coastal waters.

Newell, R.C. & E.A.S. Linley, 1984. Significance of microheterotrophs in the decomposition of phytoplankton: estimates of carbon and nitrogen flow based on the biomass of plankton communities. Mar. Ecol. Progr. Ser. 16: 105-119.

O'Connor, D.J., DiToro, D.M. & J.A. Mueller, 1987. European course on water quality and ecological modelling. Delft, The Netherlands.

Odd, N.V.M., 1988. Mathematical modelling of mud transport in estuaries. In: Dronkers, D. & van Leussen, W. (eds) Physical processes in estuaries. Springer-Verlag, Berlin. 503-531.

O'Kane, J.P., 1980. Estuarine water-quality management. Pitman, Boston.

Park, Y.C., E.J. Carpenter & P.G. Falkowski, 1986. Ammonium excretion and glutamate dehydrogenase activity of zooplankton in Great South Bay, New York. Journ. Plankt. Res., 8 (3): 489-503.

Parsons, T.R., M. Takahashi & B. Hargrave, 1984. Biological oceanographic processes. Pergamon Press, Oxford, 2nd edition.

Peierls, B., N.F. Caraco, M.L. Pace & J.J. Cole, 1991. Human influence on river nitrogen. Nature 350.

Peters, J.J. & A. Sterling, 1976. Hydrodynamique et transports de sediments de l'Escaut. In: J.C.J. Nihoul & Wollast (eds.). Project Mer. Rapport final. Bruxelles, Service de Premier Ministre. Vol. 10: 1-65.

Pond, S. & G. Pickard, 1989. Introductory dynamical oceanography. 2nd ed. Oxford, Pergamon Press.

Postma, H., 1967. Sediment transport and sedimentation in the estuarine environment. in: . Lauf (ed), Estuaries, 158-179. Am. Ass. for the adv. in Science.

Press, W.H., B.P. Flannery, S.A. Teukolsky & W.T. Vetterling, 1987. Numerical recipes: the art of scientific computing. Cambridge University press, Cambridge.

Prosser, J.I., 1990. Mathematical modeling of nitrification. In: Adv. Microb. Ecol. 11: 263-304.

Rudstam, L.G., S. Hansson & U. Larsson, 1986. Abundance, species composition and production of mysid shrimps in a coastal area of the northern Baltic Proper. Ophelia suppl. 4: 225-238.

Rudstam, L.G., 1989. A bioenergetic model for Mysis growth and consumption. J. Plankt. Res. 971-983.

SAWES, 1988. Zuurstofmodel Westerschelde. WL-rapport T257.

SAWES, 1991. Waterkwaliteitsmodel Westerschelde. WL-rapport T257.

Scholten, H, Herman, P.M.J. & De Hoop, B.J., 1990. SENECA 1.2: A Simulation ENvironment for ECological Application (Manual) Ecolmod report EM-4, DIHO/DGW, Yerseke, Den Haag. p. 150.

Scholten, H., O. Klepper, P.A.G. Hofman & S.A. De Jong, in preparation. Calculating estuarine benthic diatom primary production and community respiration with an ecosystem simulation model.

Seitzinger, S.P., 1988. Denitrification in freshwater and coastal marine ecosystems: ecological and geochemical significance. Limnol. Oceanogr. 33 (4): 702-724.

Soetaert, K. & Van Rijswijk, submitted. Spatial and temporal patterns of the zooplankton in the Westerschelde estuary.

Spitzy, A. & V. Ittekot, 1991. Dissolved and particulate organic matter in rivers. In R.F.C. Mantoura, J.M. Martin & R. Wollast (eds). Ocean margin processes in global change. Wiley & Sons, Chichester, 5-18.

Streeter, H.W. & E.B. Phelps, 1925. Study of the pollution and natural purification of the Ohio river. III. Factors concerned in the phenomena of oxidation and reaeration. Bull. U.S. Publ. Health Serv. 116.

Thomann, R.V. & J.A. Mueller, 1987. Principles of surface water quality modelling and control. New York, Harper & Row.

Tulkens, M., 1991. Ecologische studie van het meiobenthos van de Westerschelde. Licentiaatsverhandeling R.U.G., Gent.

Van Eck, G.Th.M. & N.M. de Rooij, 1990. Development of a water quality and bio-accumulation model for the Scheldt estuary. In: W. Michaelis (Ed.), Coastal and Estuarine Studies. Springer Verlag. Berlin, Heidelberg, etc. 95-104.

Van Eck, G.Th.M., N. De Pauw, M. Van den Langenbergh & G. Verreet, 1991. Emissies, gehalten, gedrag en effecten van (micro) verontreinigingen in het stroomgebied van de Schelde en het Schelde-estuarium. Water 60:164-181.

Van Spaendonk, A., J. Kromkamp & P. de Visscher, submitted. Primary production of phytoplankton in the westerschelde estuary, the Netherlands.

Vries, I.de, F. Hopstaken, H. Goossens, M. de Vries, H. de Vries & J. Heringa, 1988. GREWAQ: an ecological model for Lake Grevelingen. Rijkswaterstaat, Tidal Water division report T 0215-03.

Wetstejn L.P.M.J., 1984. Verliesprocessen voor fytoplankton. Nota DDMI-VN-301, RWS, DGW, Middelburg.

Wollast, R., 1983. Interactions in estuaries and coastal waters. In: Bolin, B. & R.B. Cook, (eds). The major biogeochemial cycles and their interactions. SCOPE.

WL-rapport, 1989. Modellering van nutrientenkringlopen in de Noordzee: EQUIPMONS en DYNAMO. Rapport Waterloopkundig Lboratorium T0234.01/T0500.03. 2 delen, augustus 1989.

Ysebaert, T. & P. Meire, 1990. Het macrozoobenthos in het sublittoraal van het mariene deel van de westerschelde (opname najaar 1988). Rapport WWE 10, R.U.G. Onderzoek in opdracht van Rijkswaterstaat, Dienst Getijdewatern.

13 Figures and tables

13.1 Figure 1. Dissolved transport: Chlorinities

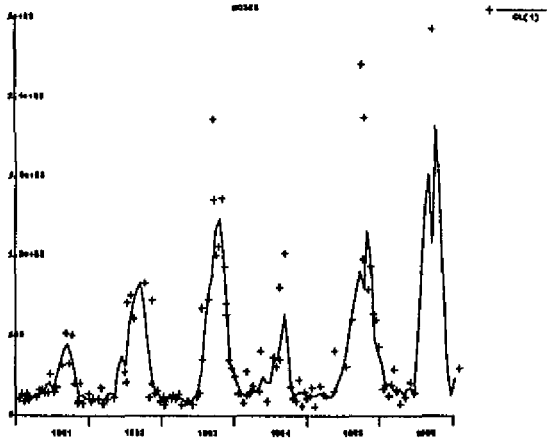

Compartment 1

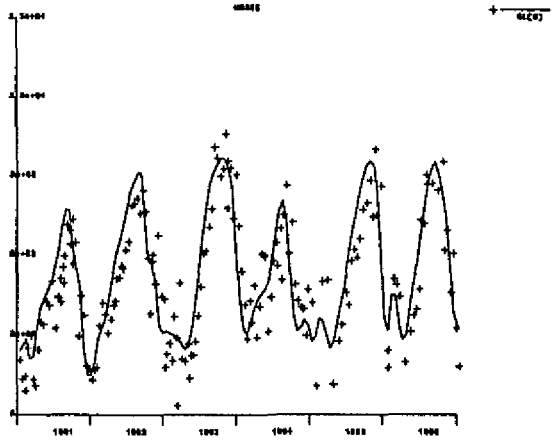

Compartment 5

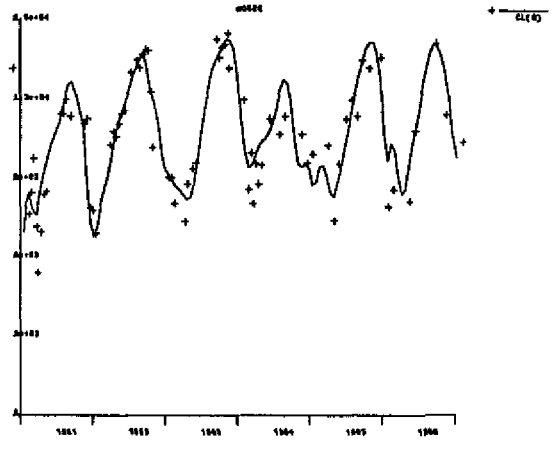

Compartment 8

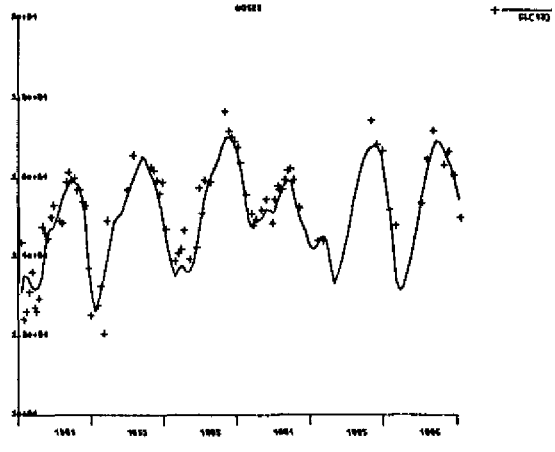

Compartment 12

(1) EXPLICIT method.

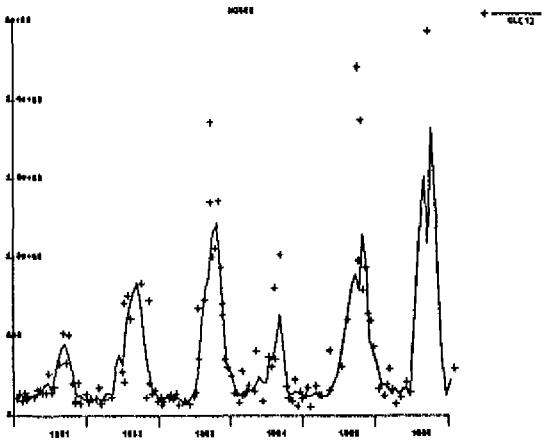

Compartment 1

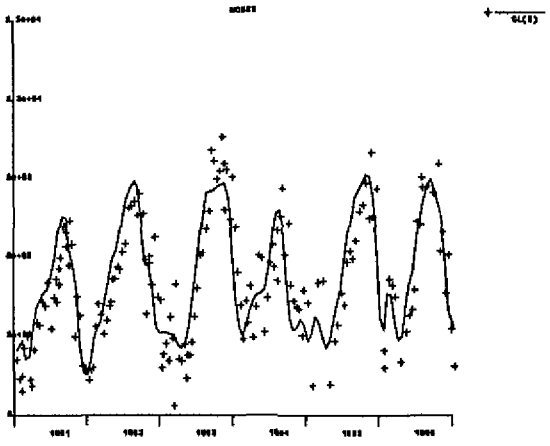

Compartment 5

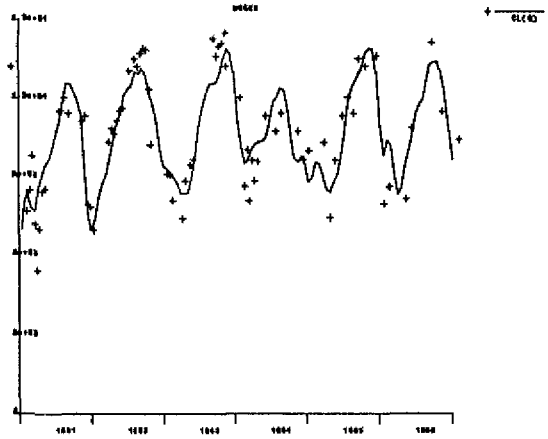

Compartment 8

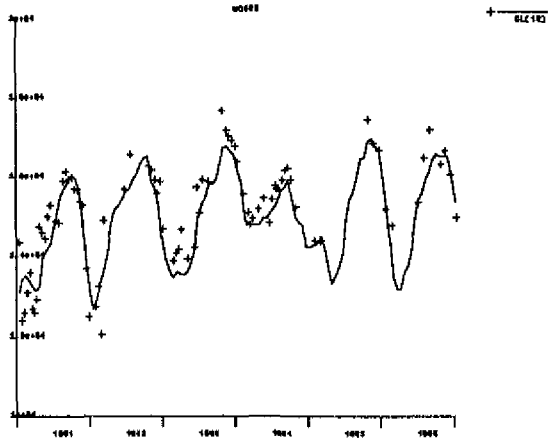

Compartment 12

(2) IMPLICIT method

13.2 Figure 2. Particulate transport: Load of suspended matter - SAWES data set

Compartment 1

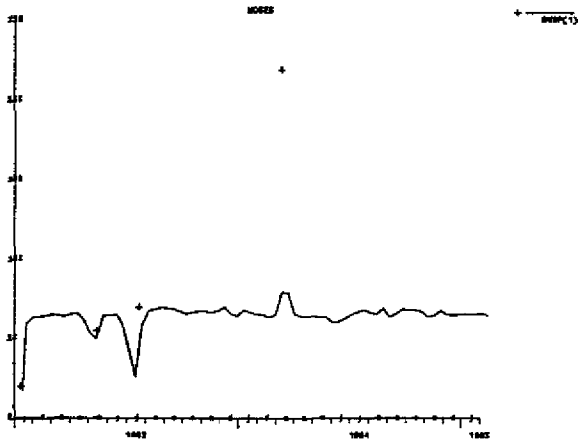

Compartment 5

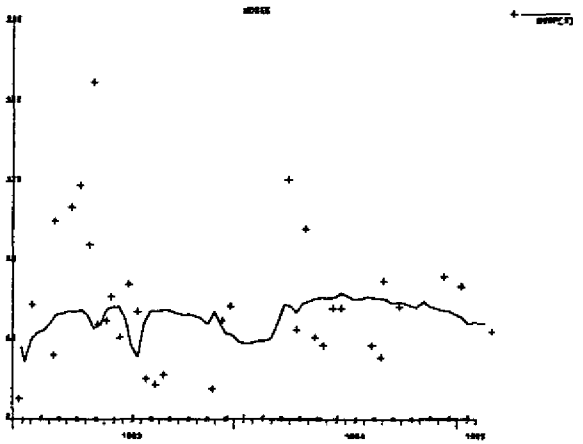

Compartment 8

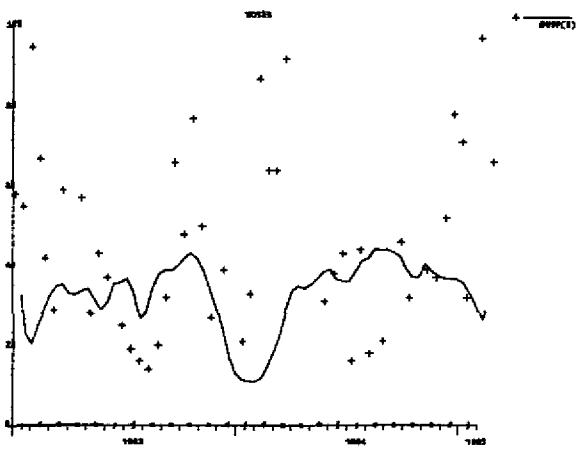

Compartment 12

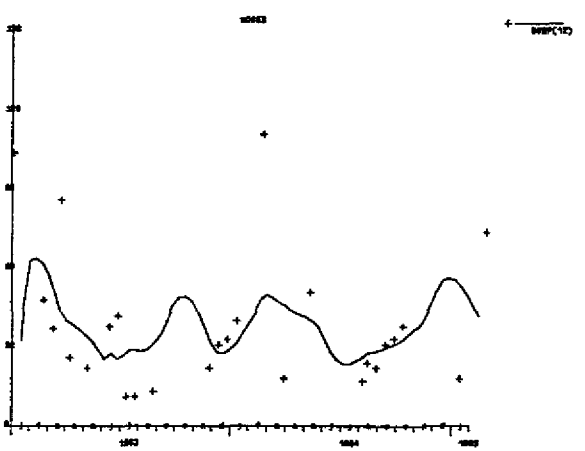

13.3 Figure 3. Particulate transport: Load of suspended matter - calculated load of suspended matter

Compartment 1

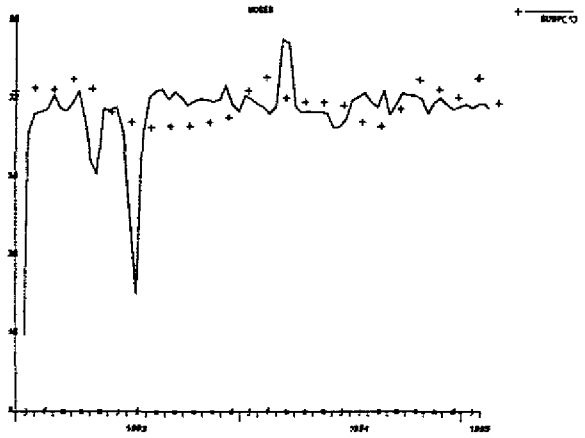

Compartment 5

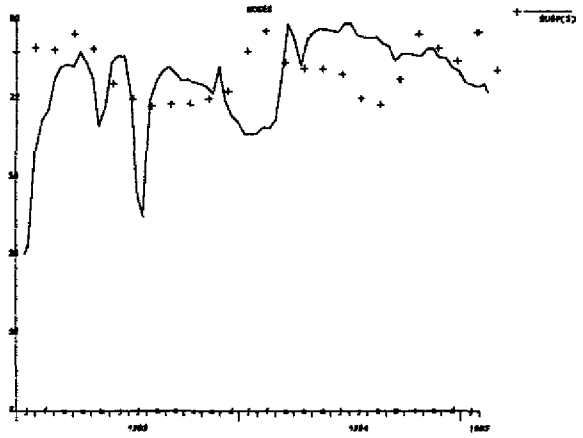

Compartment 8

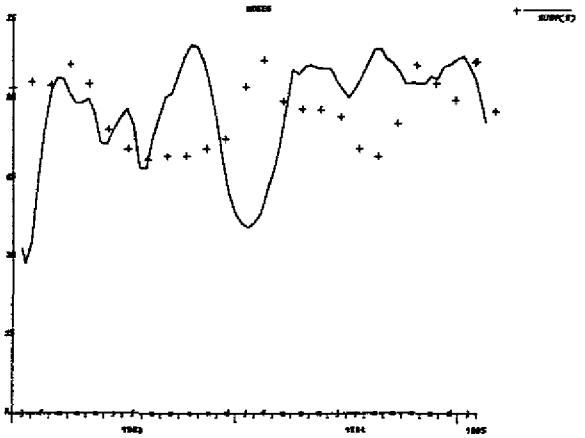

Compartment 12

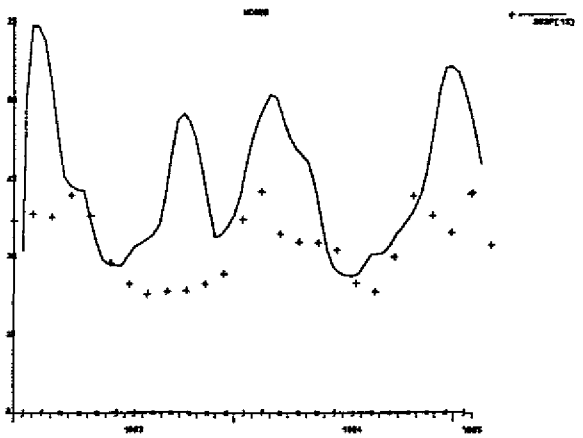

13.4 Table 1. Estimated dispersive flows

MOSES nr from	to	Dispersion flow E'	Dispersion coefficient E
fresh	1	0	0
1	2	45	91
2	3	9	16
3	4	213	224
4	5	280	188
5	6	262	130
6	7	652	153
7	8	455	75
8	9	1226	186
9	10	960	146
10	11	1921	265
11	12	1161	170
12	13	2325	381
13	sea	2120	352

13.5 Table 2. Estimated particulate (apparent) flow.

from	to	Apparent flow m^3 per sec SAWES data	calculated load
fresh	1	220	292
1	2	360	464
2	3	463	334
3	4	234	295
4	5	188	358
5	6	384	327
6	7	347	299
7	8	-57	98
8	9	99	95
9	10	126	80
10	11	188	-327
11	12	40	-76
12	13	280	264
13	sea	37	65

13.6 Table 3. Net sedimentation in subtidal

calculated from Van Maldeghem et al., 1991
Expressed in sedimentation per surface area calculated as a fraction of mean load of suspended matter in the water column.

MOSES nr	gram.m^{-2} / gram.m^{-3} / day (- erosion,+ deposition)
1	-
2	-
3	0.079
4	0.73
5	-0.049
6	0.159
7	0.327
8	-0.137
9	0.039
10	0.185
11	0.005
12	-0.132
13	0.0073

13.7 Table 4. Physical characteristics of MOSES compartments

moses nr	SURFACE in m^2*10^3 mean high	est. mean low	calc. inter-tidal	gullies	calc. sub-tidal	SURFACE in m^2*10^3 % relative to mean high inter-tidal	gullies	sub-tidal
1	3290	2733	557	734	1999	16.9	22.3	32.9
2	3360	2822	538	1199	1623	16.0	35.7	48.3
3	7159	5655	1504	2935	2720	21.0	41.0	38.0
4	3345	2531	814	1646	885	24.3	49.2	26.5
5	9106	6781	2325	3032	3749	25.5	33.3	41.2
6	19120	14548	4572	5520	9028	23.9	28.9	47.2
7	16768	10990	5778	3340	7650	34.5	19.9	45.6
8	18572	12460	6112	3380	9080	32.9	18.2	48.9
9	14200	12835	1365	7880	4955	9.6	55.5	34.9
10	39270	29874	9396	14000	15874	23.9	35.7	40.4
11	33134	28077	5057	11820	16257	15.3	35.7	49.1
12	54800	46204	8596	25420	20784	15.7	46.4	37.9
13	71314	59009	12305	37740	21269	17.3	52.9	29.8

	VOLUME m^3*10^3					VOLUME m^3*10^3		
	mean high	est. mean low	calc. inter-tidal	gullies	calc. sub-tidal	% relative to mean high inter-tidal	gullies	sub-tidal
1	33862	19834	14028	?	?	41.4	19.2	39.4
2	39452	24926	14526	?	?	36.8	20.8	42.4
3	75149	45106	30043	?	?	40.0	19.7	40.3
4	35892	22400	13492	?	?	37.6	20.5	41.9
5	89197	52488	36709	?	?	41.2	19.3	39.5
6	172926	98304	74622	27076	71228	43.2	15.7	41.2
7	247271	59962	187309	15144	44818	75.8	6.1	18.1
8	143554	76648	66906	24692	51956	46.6	17.2	36.2
9	200272	128465	71807	46252	82213	35.9	23.1	41.1
10	395028	241290	153738	90496	150794	38.9	22.9	38.2
11	369920	233638	136281	76864	156774	36.8	20.8	42.4
12	731758	483489	248269	222720	260769	33.9	30.4	35.6
13	1046875	731732	315143	371708	360024	30.1	35.5	34.4

WS characteristics vs NAP

moses nr	volume m3*10^3	surface m2*10^3	depth m	cross surf total m2*10^3	length m
1	26649	2973	9.0	4	7950
2	31957	3075	10.4	4	8300
3	59460	6387	9.3	6	9600
4	28807	2854	10.1	8	5100
5	69830	7772	9.0	14	9700
6	131128	16420	8.0	17	5950
7	86636	14380	6.0	32	5700
8	106008	14380	7.4	35	5300
9	158476	13360	11.9	39	5900
10	312588	34600	9.0	45	6900
11	300120	30300	9.9	50	6200
12	593684	49360	12.0	75	12100
13	873080	63620	13.7	80	13300

WS characteristics of boundaries

from	to	Disp length (m)	Cross section m2
fresh	1	7950	4000
1	2	8125	4000
2	3	8950	5000
3	4	7350	7000
4	5	7400	11000
5	6	7825	15750
6	7	5825	24750
7	8	5500	33500
8	9	5600	37000
9	10	6400	42000
10	11	6550	47500
11	12	9150	62500
12	13	12700	77500
13	sea	13300	80000

MOSES

Addendum I

Data gathering and data modification

Karline Soetaert, Peter M.J. Herman & Huub Scholten

Netherlands institute of ecology
Centre for estuarine and coastal ecology

Ecolmod rapport EM-3

Table of contents

1 Introduction

Building a global ecosystem model requires a lot of data to be used as forcing functions or for calibration/validation purposes. The data set used in MOSES consists for a great deal of data gathered for the SAWES model (SAWES, 1991). Some data were obtained from SMOES (Klepper, 1989), from the DIHO (NIOO) or from the State University of Ghent. As the data obtained from SAWES required a specific treatment, they are discussed in a separate chapter.

2 The SAWES data set

The data set used in the SAWES model (SAWES, 1991) was obtained from Van Eck and Schouwenaar (Wattel & Schouwenaar, 1991). It consists of different kinds of files:

2.1 Raw data

2.1.1 Concentration per compartment

335 files contained measured concentrations of various substances at several sampling stations for the period 1980 to 1988 (and some of 1970-1980). An accompaying file contained the transposed positions of these stations with respect to the fixed volume reference scheme.

The SAWES data set consisted of the station numbers 1-4, 7, 30, 40, 60, 70, 80, 90, 101-103, 110-114, 118, 120, 122, 124, 130, 135-136, 138, 140. (Wattel & Schouwenaar, 1991). Distances of these stations to the freshwater boundary of the model are given in de Jong (1988).

Following parameters were provided (with their code, Wattel & Schouwenaar, 1991):
Temperature (P000010), Flows (P000061), Oxygen concentration (P000300), biochemical oxygen demand (P000310), chemical oxygen demand (P000340), total organic carbon (P000680), dissolved organic carbon (P000681), suspended matter (P000530), NH4N (P0006080), NO2 (P000613), NO3 (P000614), Kjehldahl N (P000625), NO3NO2 (P000630), PO4P (P000671), Cl (P000940), dissolved Si (P001140), Chl a (P032230) and total P (P070505).

Not all parameters were measured at all stations.

2.1.2 Waste loads

Eleven files (one per substance) contained yearly average wastes of various origin. Total wastes as well as the contributions of poldars, channels, communal wastes, industrial wastes and precipitation were provided.
It concerned following substances: Flows, biochemical oxygen demand, chemical oxygen demand, suspended matter, NO3NO2, Kjehldahl N, total nitrogen, dissolved Si, PO4P, total P.

2.1.3 Physical characteristics of the compartments

This data set consisted of four files as described in de Jong, 1988.
It contained the surfaces and volumes at certain levels above or below NAP in the 14 SAWES compartments, the surface at mean high water level in the 14 compartments, the total surface, volume at NAP, mean depth, cross surface and dispersion length.

2.1.4 Flows

Monthly net flows between compartments and across the boundaries were provided for the period 1980 to 1988.

2.2 Modification of the SAWES data set

In the current ecological model of the Westerschelde, SAWES compartment 6 and 7 were combined into one compartment. Thus only 13 MOSES compartments were distinguished as opposed to 14 SAWES compartments. This was taken into account when converting the SAWES data set.

2.2.1 Concentration per compartment

The 335 SAWES files, one per station and per substance were converted into 18 MAT files usable in MOSES. The resulting files, one per substance, consist of a mean concentration per compartment.
This was achieved as follows:
Using the transposed location of each station (with respect to the fixed volume reference scheme), the sampling was assigned to one of the MOSES compartments. Distances of the MOSES compartment edges towards the fresh boundary of the model were found in de Jong (1988). However, as not all samplings were transposed missing values were assigned to the compartment of the fixed reference scheme (i.e. as if sampling occurred at mean tide). Concentrations per compartment were calculated as mean values rather than interpolating them to the middle of each compartment (as was done in the Oosterschelde by Klepper, 1989). This approach was chosen as (1) the compartments are assumed to be homogeneous with respect to biological and chemical characteristics and (2) when all measured values ly on the same side of the compartment, calculating concentrations at the middle of the compartment becomes an extrapolation exercise rather than interpolation. This can result in severe deviations.

Due to the transposition, some stations were positioned outside the 13 MOSES compartments. They were used as boundary data. Similarly, some data at the boundaries proved to belong to one of the MOSES compartments.

Temperature data from 1986 on were unavailable for the most upstream compartments. As this data set is used as a forcing function, the simulation was restricted to the years previous to 1986. Moreover, temperature data of compartment 6 were too broadly spaced in time. This was solved by taking the average of two adjacent compartments whenever these temperatures were available.

2.2.2 Waste loads

Waste loads were yearly averages and a distinction was made between Belgian and Dutch data. In the modified MOSES data set, no distinction was made between these two sources. The SAWES flow data (monthly values) were used to calculate net waste flows per month (see section on flows). In MOSES, this data set is combined with the yearly averaged data set to calculate monthly wastes instead of yearly averages. Total waste loads as well as the loads in poldars, channels, communal wastes, industrial wastes and precipitation are provided.

2.2.3 Physical characteristics of the compartments

These data were used to calculate the surface and volumes of the intertidal, subtidal areas and the gullies in each compartment. Data on total compartment volume, surface, mean depth, and cross surface were used as such. Total length of compartments was calculated from de Jong (1988). Cross sectional areas between compartments and at the boundaries were obtained calculated as the mean of cross sectional surface of adjacent compartments as in SAWES (1991). Dispersion length across the boundaries was defined as the mean of total length of the adjacent compartments. Dispersion length across the upstream boundary of the first compartment and across the downstream boundary of the last compartment were taken equal to

the compartment length.
The intertidal surface per compartment was calculated as the area at mean high water - area at mean low water. Gullies were defined as those parts deeper than 10 meter. Subtidal areas and volumes consist of the remains. Data at mean high water were present and defined as 2.35 meter above NAP in de Jong (1988). Data at mean low water were interpolated and mean low water was defined as 2.15 meter (Terneuzen), 2.30 meter (Hansweert) and 2.39 meter (Bath) below NAP (from Bollebakker, 1985)
The data set was accurate for the Dutch part of the Schelde, but insufficient for the Belgian part. More specifically, data on the surfaces and volumes at 10 meter below NAP (defined as gullies) for the different compartments were missing. A request was sent to the 'waterbouwkundig lab' at Borgerhout, Belgium. Five maps with detailed information of the Belgian part of the Schelde were obtained. From these the required information was extracted.

2.2.4 Flows

Monthly net flows between compartments and across the boundaries were provided for the period 1980 to 1988. This data set was converted into MAT format and used to calculate monthly waste flows : the net flow at the downstream boundary of a compartment equals the sum of net upstream flow and input in the compartment (waste). Thus monthly waste flow in compartment i was calculated as $Q_{(i,i+1)} - Q_{(i-1,i)}$, with $Q_{(i,i+1)}$ the monthly averaged net flow between compartment i and i+1. The data obtained in this way were tested for consistency with the yearly averaged waste flows.

3 Other data sets

3.1 Irradiance

Irradiance data are used from SMOES (Klepper, 1989). They are averages of six stations around the Oosterschelde.

3.2 Phytoplankton and concurrent chemical data

Data on phytoplankton primary production were obtained for the period '89 - '90 from Van Spaendonck (Van Spaendonck et al., submitted). It are primary production, pMAX and alpha values. Values measured in 1991 for integrated production and coefficients of the Eilers-Peeters (1988) model (Kromkamp et al.) were used for the parameterisation of the light-limited production in MOSES (see ???). Other data on primary production will become available from J. Kromkamp (NIOO, CECE).

3.3 Microbial processes

Microbial activity is currently being investigated by N. Goosen (NIOO, CECE). Data will be incorporated in the MOSES data set.

3.4 Zooplankton and concurrent chemical data

A zooplankton data set and concurrent chemical data were obtained from Soetaert (Soetaert & Van Rijswijk, submitted) for the period '89-91.
Zooplankton dry weight is divided into mesozooplankton, microzooplankton and benthic larvae dry weight. Mesozooplankton biomass estimates are most reliable as they are obtained from length-weight regressions. Dry weights of benthic larvae and microzooplankton should be considered with caution as they are derived from density data, using crude conversion factors. Moreover, the 'microzooplankton' only consists of those individuals larger than 55 um, the used mesh (mainly Rotatoria and Noctiluca).
The chemical data are salinity, temperature, chlorophyll, DOC, POC, suspended matter, NH4N, NO3NO2, Si, oxygen concentration and oxygen

saturation. From 89 to 1990, only nitrate and not nitrite was measured ; from 1991 on, both were quantified. NO2 proved to be on average 5 % of total NO3NO2 concentration. This value was used to convert the NO3 values to total nitrate + nitrite concentration.

These data consisted of non-transposed values. However, the time of sampling relative to high water was given. Transposing to the fixed volume frame was done with a formula, modified from van Maldegem (1988):

$$Xt = Xm - GW(Xm)/2*\cos(t/T*2pi)$$

with

Xm = distance of sampling station to Schelle
GW(Xm) = tidal excursion (interpolated from van Maldegem, 1988)
t/T = time relative to high water
Xt = transposed position of sample

The influence of physical factors (wind, slack water, spring tide) was not considered.

As with the SAWES data, some values were outside the boundaries after transposing. They were used as boundary conditions.

Data on zooplankton grazing and secondary production will become available (Kromkamp & Goosen, Escaravage, Soetaert, all from the NIOO-CECE; Tackx from the V.U.B., Belgium).

3.5 Macrobenthos

A time series study of total macrobenthic biomass (ash-free dry weight) from 78 to 85 was performed at three intertidal stations (in MOSES intertidal compartments 1 to 10) by Heip et al. (1986).
Ysebaert & Meire (1990) performed an extensive study of inter- and subtidal macrobenthos in september 1988. Stations were positioned in MOSES intertidal compartments 1, 2, 4 and 5. Only values for intertidal stations were included into MOSES.
In Jansen et al. (1989) biomass values of two stations on 5 occasions can be found (intertidal compartments 4 and 9).
Craeymeersch delivered data from subtidal and channel stations in (pelagic) compartments 6 to 13 (project BIOMON). Samples were from 3-9 september 1990. As subtidal and channel environments are not considered in MOSES, they were not modified. Interrtidal BIOMON data from spring '91 and fall '91 will become available from the same author.

3.6 Hyperbenthos

Data were obtained from Mees & Hamerlynck (submitted). It concerns a transect in december 1988, comprising compartments 6 to 13. Data from 14 stations ranging from Vlissingen to Bath, taken in april 1990, august 1990 and december 1990 were obtained from Mees (from Dewicke, 1991). A year cycle of april 1990 to march 1991 in two stations (vlissingen and Bath) consisted only of density data. Other data will become available from the same authors.

3.7 Suspended matter

The data set on suspended load proved to be very erratic and there was even no whole year with data for the entire westerschelde. Moreover, the data set itself showed a large degree of scatter, as the sampling time with respect to the phase of the tide was not taken into account when transforming the data. For the ecosystem model, it appeared desirable to remove this tide-induced variation and to obtain an adequate description of suspended matter in the estuary with as few parameters as possible. It was thus decided to calculate a regression of suspended matter on freshwater flow intensity, taking into account the position with respect to the schematisation. On the average, the suspended load increased from the freshwater boundary towards compartment 2 and then declined steadily towards the sea. Thus, if x represents the distance to Schelle and FLOW the average compartment flow, the regression obtained was (Figure 1):

SUSP = 300.0*ln(X) - 15.92*(ln(X))^2 + 0.016*FLOW*ln(X) - 0.062* FLOW - 1331.5.

(1)

3.8 Benthic diatoms

Concentrations of chlorophyll a, b, phaeophytine a and b (µg/gram dry weight) and the water content of the sediment were provided from D. de Jong (DGW-Middelburg) for januari to september 1991 in various stations along the Dutch Westerschelde. They were converted to mean concentrations per MOSES benthic compartment.

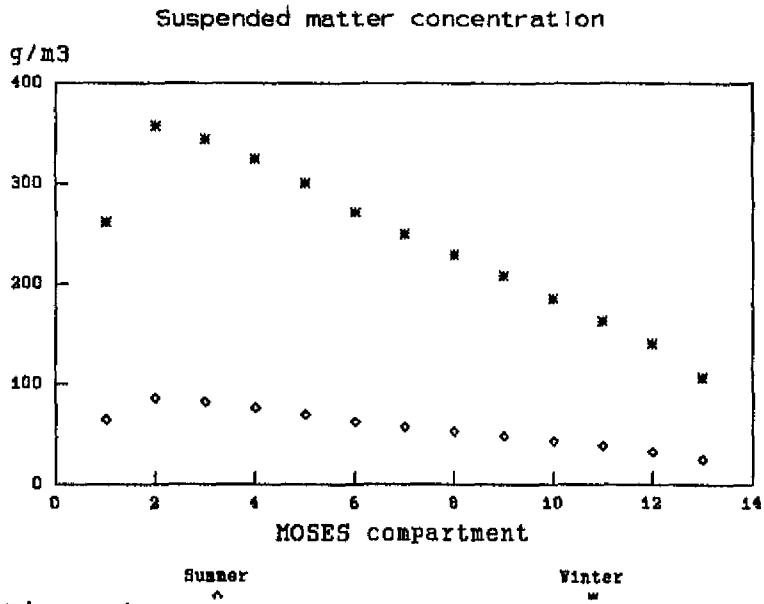

Figure 1. Load of suspended matter for a typical summer and winter situation.

4 Table: Summary of MAT files in MOSES

Name	Description	Source	Use
(1) Pelagic data			
FTEMP	Temperature (degrees celsius)	SAWES	F
FLOW	Freshwater flow ($m^3.sec^{-1}$), monthly data	SAWES	F
FMESO	Mesozooplankton dry weight ($g.^{-3}$)	CEMO	F
FMICRO	Microzooplankton dry weight ($g.m^{-3}$)	CEMO	F
LICHT	Mean light intensity at 3 ES stations ($W.m^{-2}$)	SMOES	F
WFLOW	Waste flow, yearly averages ($m3.day^{-1}$)	SAWES	W
WFLOWmn	Waste flow, monthly data ($m3.day^{-1}$)	SAWES	W
WNH4	NH4 load in wastes (kg N.day-1) (1)	SAWES	W
WNITR	NO3+NO2 load in wastes (kg $N.day^{-1}$) (1)	SAWES	W
WSOLSi	Soluble Silicate in wastes (kg $Si.day^{-1}$) (1)	SAWES	W
WBOD	BOD in wastes (kg $O.day^{-1}$) (1)	SAWES	W
BOD5	Biochemical oxygen demand at 20 C (g $O.m^{-3}$)	SAWES	BF
SEAZOO	Meso- and microzooplankton dry weight in sea	CEMO	BF
CHLOR	Chlorophyl content ($mg.m^{-3}$)	SAWES	BF
FDIAFRAC	Diatom fraction at the boundaries (-)	SMOES	BF
CL	Chloride ($g.m^{-3}$)	SAWES	B,O
NH4	NH4 (g $N.m^{-3}$)	SAWES	B,O
NITR	NO3+NO2 (g $N.m^{-3}$)	SAWES	B,O
SOLSi	Soluble silicate (g $Si.m^{-3}$)	SAWES	B,O
OXYGEN	Oxygen (g $O.m^{-3}$)	SAWES	B,O
MESOZOO	Mesozooplankton dry weight ($g.m^{-3}$)	CEMO	O
MICRZOO	Microzooplankton dry weight ($g.m^{-3}$)	CEMO	O
TOC	Total organic carbon (g $C.m^{-3}$)	SAWES	O
PMAX	Max primary production (mg C.mg $chl^{-1}.h^{-1}$)	CEMO	O
PPROD	primary production (mg $C.m^{-2}.day^{-1}$)	CEMO	O
(2) Benthic data			
FDRYQ	Fraction of time the flats are dry (-)	SMOES	F
FSPAWN	Trigger function for spawn condition Susp. f.	-	F
BENCHLa	Sedimentary Chl a (µg chl.g dry $weight^{-1}$)	DGW	O
MACRO	Macrobenthos ash-free dry weight ($g.m^{-2}$)	CEMO-RUG	O
SUSPFRAC	Fraction of benthos that is suspension feeder	CEMO	O
HYPER	Hyperbenthos ash-free dry weight ($g.m^{-2}$)	RUG	O
(3) Used for the calibration of the transport module			
NSED	Net sedimentation ($g.m^{-3}.day^{-1}$)	SAWES	O,F(2)
OWNSUSP	Suspended matter ($g.m^{-3}$) (formula 1)	MOSES	O
(4) Not (yet) used in MOSES			
WKJELN	Kjeldahl nitrogen in wastes (kg $N.day^{-1}$) (1)	SAWES	-
WTOTN	Total nitrogen load in wastes (kg $N.day^{-1}$) (1)	SAWES	-
WPO4	PO4 load in wastes (kg $P.day^{-1}$) (1)	SAWES	-
WTOTP	Total phosporous (kg $P.day^{-1}$) (1)	SAWES	-
COD	Chemical oxygen demand at 20 C (g $O.m^{-3}$)	SAWES	-
DOC	Dissolved organic carbon (g $C.m^{-3}$)	SAWES	-
SUSP	Suspended matter ($g.m^{-3}$)	SAWES	-
KJELN	Kjeldahl nitrogen (g $N.m^{-3}$)	SAWES	-
NO2	NO2 (g $N.m^{-3}$)	SAWES	-
NO3	NO3 (g $N.m^{-3}$)	SAWES	-
PHOS	Total phosporous (g $P.m^{-3}$)	SAWES	-
PO4	PO3 (g $P.m^{-3}$)	SAWES	-
CHLOR_89	Chlorophyl content ($mg.m^{-3}$)	CEMO	-
DOC_89	Dissolved organic carbon (g $C.m^{-3}$)	CEMO	-
NH4_89	NH4 (g $N.m^{-3}$)	CEMO	-
NITR_89	NO3+NO2 (g $N.m^{-3}$)	CEMO	-
SOLSi_89	Soluble silicate (g $Si.m^{-3}$)	CEMO	-
OXYG_89	Oxygen (g $O.m^{-3}$)	CEMO	-
OX%_89	Oxygen saturation (%)	CEMO	-

SAL_89	Salinity (‰.)	CEMO	-
SECH_89	Secchi visibility (cm)	CEMO	-
SUSP_89	Suspended matter ($g.m^{-3}$)	CEMO	-
TEMP_89	Temperature (degrees celsius)	CEMO	-
ALPHA	alpha values of primary production ($.chl^{-1}$)	CEMO	-
BENTLAR	Dry weight of benthic larvae ($\mu g.m^{-3}$)	CEMO	-
COPEPOD	Dry weight of copepods ($\mu g.m^{-3}$)	CEMO	-
EVAPOR	evaporation at Vlissingen ($mm.month^{-1}$)	SMOES	-
PRECIP	Precipitation at Vlissingen ($mm.month^{-1}$)	SMOES	-
BENCHLb	Sedimentary Chl b (μg chl.g dry $weight^{-1}$)	DGW	-
BENH2O	Sedimentary water content (%)	DGW	-
BPHAEO_a	Sedimentary phaeophyt a ($\mu g.g$ dry $weight^{-1}$)	DGW	-
BPHAEO_b	Sedimentary phaeophytb ($\mu g.g$ dry $weight^{-1}$)	DGW	-

F = forcing function, W = Waste load, B = boundary condition, BF = boundary condition imposed as a forcing function, O = observed data, - = not used in MOSES.

SAWES = obtained from Van Eck & Schouwenaar (SAWES, 1990); SMOES = from the ecosystem model of the Easterscheldt (Klepper, 1989); MOSES = this model; CEMO = NIOO-centrum voor Estuariene en Mariene Oecologie; RUG = Rijksuniversiteit Gent; D.G.W. = Rijkswaterstaat, dienst getijdenwateren.

[1] Wastes are yearly averages and expressed as total loads, loads in poldars, channels, communal wastes, industrial wastes and in precipitation.

[2] Calculated from sediment transport values in SAWES (1991)

5 References

de Jong, H., 1988. Berekening van inhouden en oppervlaktes van de Schelde en Westerschelde t.b.v. SAWES. GWAO-88.1314.

Bollebakker, G.P., 1985. Ijking en verificatie van het een-dimensionaal mathematisch model IMPLIC voor het scheldebekken met bodemligging 1981. Nota WWKZ-85.V006.

Dewicke, A., 1991.

Heip, C., R. Herman & J. Craeymeersch, 1986. Diversiteit, densiteit en biomassa van het macrobenthos in de westerschelde. Rapport R.U.G. in opdracht van de dienst getijdewateren, RWS, Nederland.

Jansen, C.R., E. Boel, R. Herman & M. Vincx, 1988. Diversiteit, densiteit en biomassa van het macrobenthos in de westerschelde: 1986-1988. Rapport R.U.G. in opdracht van de dienst getijdewateren, RWS, Nederland.

Klepper, O, 1989. A Model of Carbon Flows in Relation to Macrobenthic Food Supply in the Oosterschelde Estuary (S.W. Netherlands). Ph. D. thesis, University of Wageningen, Wageningen, 1-270.

Mees, J. & O. Hamerlynck, submitted. Spatial community structure of the permanent hyperbenthos of the schelde-estuary and the adjacent coastal waters.

Ministerie van openbare werken, bestuur der waterwegen antwerpse zeedienSten hydrografie. Hydrografishe kaarten van het Belgische deel van de Schelde.

SAWES, 1991. Waterkwaliteitsmodel Westerschelde. SAWES nota 91.01. T257.

Soetaert, K. & P. Van Rijswijk, submitted. Spatial and temporal patterns of the zooplankton in the Westerschelde estuary.

Van Spaendonck, A., J. Kromkamp & P. de Visscher, submitted. Primary production of phytoplankton in the westerschelde estuary, the Netherlands.

Wattel, G. & A. Schouwenaar, 1991. De bestanden met hieruit de berekende

belasting van het schelde estuarium over de periode 1980-1988. Nota GWWS-89.648, GWWS-89.646, GWWS-90.13150, GWWS-91.13054.

van Maldegem, D., 1988. Verzeilen van de immissiegegevens van het oppervlaktewater van het schelde estuarium over de periode 1975 t/m 1986. GWAO-88.1267.

Ysebaert, T. & P. Meire, 1990. Het macrozoobenhtos in het sublittoraal van het mariene deel van de westerschelde (opname najaar 1988). Rapport WWE 10, RUG.